

Alternation of Singlet and Triplet States in Carbon-Based Chain Molecules and Its Astrochemical Implications. Results of an Extensive Theoretical Study

Ioan Bâldea^{*,†,‡}

[†]*Theoretische Chemie, Universität Heidelberg, Im Neuenheimer Feld 229, D-69120
Heidelberg, Germany*

[‡]*Institute of Space Sciences, National Institute of Lasers, Plasma and Radiation Physics,
RO 077125, Bucharest-Măgurele, Romania*

E-mail: ioan.baldea@pci.uni-heidelberg.de

Abstract

A variety of homologous carbon chains (HC_nH , HC_nN , C_nS , C_nO , and OC_nO) are found to exhibit an appealing even-odd effect. Chains containing a number of carbon atoms of a certain parity possess singlet ground states, while members of opposite parity have triplet ground states. From a general perspective, it is important that this even-odd effect confounds straightforward chemical intuition. Whether the most stable form is a triplet or a singlet is neither simply related to the fact that the species in question is a “normal” (closed-shell, nonradical) molecule nor a (di)radical or to the (e.g., cumulene-type) C-C bond succession across the chain. From a computational perspective, the present results are important also because they demonstrate that electron correlations in carbon-based chains are extremely strong. Whether the

“gold-standard” CCSD(T) (coupled-cluster expansions with single and double excitations and triple excitations corrections) framework suffices to describe such strongly correlated systems remains an open question that calls for further clarification. Most importantly for astrochemistry, the present results may explain why certain members are not astronomically observed although larger members of the same homologous series are detected; the missing species are exactly those for which the present calculations predict triplet ground states.

Keywords

carbon chains; ab initio methods; molecular electronic structure; interstellar matter; singlet-triplet interplay

1 Introduction

Linear carbon chains represent a field of great current interest for fields ranging from (bio-)molecular electronics to astrochemistry. Until the advent of nanoelectronics^{1–4} such molecules were often of little interest for (terrestrial) laboratory studies and practical applications. Cyclic or combined ring-chain structures are usually more stable energetically than linear isomers.⁵ This explains the scarcity of available information on carbon-based chains. For the vast majority of the molecular species to be considered in the present paper the NIST database contains no entries. A number of molecules comprising carbon chains were observed in the past decades in cold interstellar and circumstellar clouds.^{6–21}

The identification of the type of ground state (which is the most stable isomer?) of the various molecular species of interest represents the most basic information, also needed to correctly understand a certain extraterrestrial environment and to simulate its astrochemical evolution. In the present paper, we addressed this issue by examining in detail representative homologous series of carbon-based linear chains (HC_nH , HC_nN , C_nS , C_nO ,

and OC_nO). We found that, by successively adding atoms to the molecular backbone of all these astrochemically relevant families of carbon-based chains with an even number of electrons, the most stable form systematically switches back and forth between singlet and triplet isomers. Rephrasing, we will show below that the most stable state of members of a certain parity (even or odd) of a chain family is a singlet (ground) state, while members of opposite parity (odd or even, respectively) have a triplet ground state. One should note at this point that the present finding that triplet states of carbon-based chains can be surprisingly lower in energy and lie below singlet states contradicts some recent studies done in the astronomical/astrophysical community.^{22,23} Those studies explicitly²⁴ or implicitly²² claimed (see Section 3.8 and the SI) that all carbon chains of the type considered in the present paper possess a singlet ground state.

Noteworthy, the even-odd singlet-triplet alternation²⁵ extensively discussed in this paper is qualitatively different from all other even-odd effects (*e.g.*, in multilayers,²⁶ self-assembled monolayers,²⁷ quantum dot arrays,^{28–31} molecular electronic devices^{2,3}) known since the early days of quantum mechanics.^{32–35} In those cases, it is merely a certain property rather than the very nature of the ground state that exhibits alternation.

2 Methods

All quantum chemical calculations done in conjunction with the present study were performed by running the GAUSSIAN 16 suite of programs³⁶ on the bwHPC platform.³⁷ Optimized geometries ($\mathbf{R}_{S,T}$) of all singlet (S) and triplet (T) carbon-based chains considered in this paper were obtained from DFT calculations using the B3LYP hybrid exchange functional and, unless otherwise stated (*cf.* Tables S1–S4 of the SI) the largest Pople 6-311++g(3df, 3pd) basis sets. In all cases, we checked that all frequencies were real.

For the largest molecular species of each homologous series, we also performed state-of-the-art calculations based on coupled-cluster (CC) expansions with single and double exci-

tations (CCSD) supplemented by perturbative treatment of triple excitations (CCSD(T)).³⁸ For triplet states, we employed the unrestricted and restricted open shell formalism for DFT calculations and CC-calculations, respectively. More technical details are presented in Section S1 of the SI.

Enthalpies of formations $\Delta_f H^0$ (Tables 1, 3, 5, 7, and 9) were computed using the standard methodology.³⁹ For comparison purposes (*cf.* Section 3.8), along with the values obtained within a DFT/B3LYP/6-311++g(3df, 3pd) approach we also estimated enthalpies of formation using the CBS-QB3 protocol as implemented in GAUSSIAN 16, which are shown in Tables S1–S4 of the SI.

A thermochemical analysis may not be sufficient for molecules of interest for astrochemistry, where single-particle (kinetic) effects also deserve consideration. Therefore, in addition to enthalpies of formations for both the lowest singlet and triplet electronic ground states, we also report values estimates for the singlet-triplet separation energies $\Delta \equiv \mathcal{E}_T - \mathcal{E}_S$. They were obtained as differences of the corresponding total molecular energies $\mathcal{E}_{S,T}(\mathbf{R})$ at the pertaining molecular energies ($\mathbf{R} = \mathbf{R}_{S,T}$). For all the families of carbon chains considered (Tables 2, 4, 6, 8, and 10), we present values of both adiabatic and vertical singlet-triplet separation energies. The adiabatic value

$$\Delta_{adiab} \equiv \mathcal{E}_T(\mathbf{R}_T) - \mathcal{E}_S(\mathbf{R}_S) \quad (1)$$

represents the difference between the triplet (T) and singlet (S) energies computed at the molecular geometries $\mathbf{R} = \mathbf{R}_{S,T}$ optimized for the singlet (\mathbf{R}_S) and the triplet (\mathbf{R}_T) isomers. The two distinct vertical values $\Delta_{S,T}$

$$\Delta_S \equiv \mathcal{E}_T(\mathbf{R}_S) - \mathcal{E}_S(\mathbf{R}_S) \quad (2a)$$

$$\Delta_T \equiv \mathcal{E}_T(\mathbf{R}_T) - \mathcal{E}_S(\mathbf{R}_T) \quad (2b)$$

correspond to differences between the triplet (T) and singlet (S) energies taken at the same molecular geometry (either singlet \mathbf{R}_S or triplet \mathbf{R}_T).

According to Equation (2), positive Δ -values imply that singlet isomers are more stable than triplet isomers; negative Δ -values correspond to triplets more stable than singlets. The inspection of the various Δ 's presented in the next sections reveals that cases exist — *e.g.*, the even-member HC_{2k}H chains, *cf.* Table 2 and the odd-member HC_{2k+1}N chains, *cf.* Table 4, whose most stable isomers are singlets with polyyne structure — for which the values of Δ_S and Δ_T significantly differ from each other. By virtue of Equation (2), for such molecular species the corresponding singlet and triplet isomers are characterized by significantly different geometries. In many other cases — like the longer odd-members HC_{2k+1}H chains whose most stable isomers are triplets possessing a cumulenic structure, *cf.* Table 2 — the values of Δ_S and Δ_T are almost equal.

Given the fact discussed in detail below that, depending on the parity of the number of atoms, singlet or triplet isomers are more stable, it makes sense to also consider vertical singlet-triplet splitting energies $\Delta_{m.s.}$ at the geometry of the most stable (acronym *m.s.*) isomer, which are defined as

$$\Delta_{m.s.} = \begin{cases} \Delta_S \equiv \mathcal{E}_T(\mathbf{R}_S) - \mathcal{E}_S(\mathbf{R}_S) > 0 & \text{if } \mathcal{E}_S(\mathbf{R}_S) < \mathcal{E}_T(\mathbf{R}_S) \quad (\text{singlet more stable than triplet}) \\ \Delta_T \equiv \mathcal{E}_T(\mathbf{R}_T) - \mathcal{E}_S(\mathbf{R}_T) < 0 & \text{if } \mathcal{E}_T(\mathbf{R}_T) < \mathcal{E}_S(\mathbf{R}_T) \quad (\text{triplet more stable than singlet}) \end{cases} \quad (3)$$

Values of $\Delta_{m.s.}$ for the various families of chains considered are depicted in Figures 2c, 4c, 6c, 8c, and 10c.

In addition to DFT/B3LYP estimates of the singlet-triplet separations Δ , we also report Δ -values deduced by performing *ab initio* CCSD and state-of-the-art CCSD(T) calculations. To facilitate comparison with results of other elaborate *ab initio* electronic structure approaches that could (or should, *cf.* Section 3.9) be applied in subsequent studies, the CCSD and CCSD(T) Δ -estimates reported here (*cf.* Tables 2, 4, 6, 8, and 10) do not include corrections due to zero-point motion. One should mention in this context that zero-point energy

corrections within *ab initio* approaches like CCSD and CCSD(T) are very challenging; they require costly numerical frequency calculations. Currently feasible studies of this kind are restricted to *closed*-shell (that is, singlet but not triplet) species and smaller molecular sizes.⁴⁰ As a trade-off between accuracy and computationally demanding *ab initio* frequency calculations, zero-point energy corrections can be applied within the DFT/B3LYP approach. Such estimates are indicated by label *corr* in Tables 2, 4, 6, 8, and 10. So, values labeled “B3LYP (corr)” in those tables refer to results of DFT/B3LYP calculations including corrections due to zero-point motion while values labeled “B3LYP” were obtained from DFT/B3LYP calculations without zero-point energy corrections. The rather minor differences between these two corrected and uncorrected values visible in Tables 2, 4, 6, 8, and 10 suggest that, in spite of the enormous computational effort, the benefit of CCSD(T) numerical frequency calculations, even if implemented, would be questionable.

3 Results and Discussion

In the sections that follow we will extensively analyze the most representative families of carbon-based chains found in interstellar molecular clouds. For each family, we investigated molecular sizes exceeding the longest chain astronomically observed; the latter is indicated in the corresponding table caption. Depending on their chemical composition, the chains considered are either “normal” (*i.e.*, closed-shell, nonradical) or diradical⁴¹ molecules characterized by polyyne- or cumulene-type structures.

3.1 HC_{*n*}H Homologous Series

The members with an even number ($n = 2k$) of carbon atoms of this family, HC_{2*k*}H ($k = 1, 2, \dots$), which we first consider, are polyynes wherein single C–C and triple C≡C carbon-carbon bonds alternate across the chain backbone H–C≡C–...≡C–H. This alternation is illustrated by the results shown in Figure 1a, which depicts the Wiberg bond order indices

calculated for the singlet HC_{12}H chain. All valence electrons form pairs between adjacent atoms, and this typically renders the singlet state of the chain to be the most stable form.

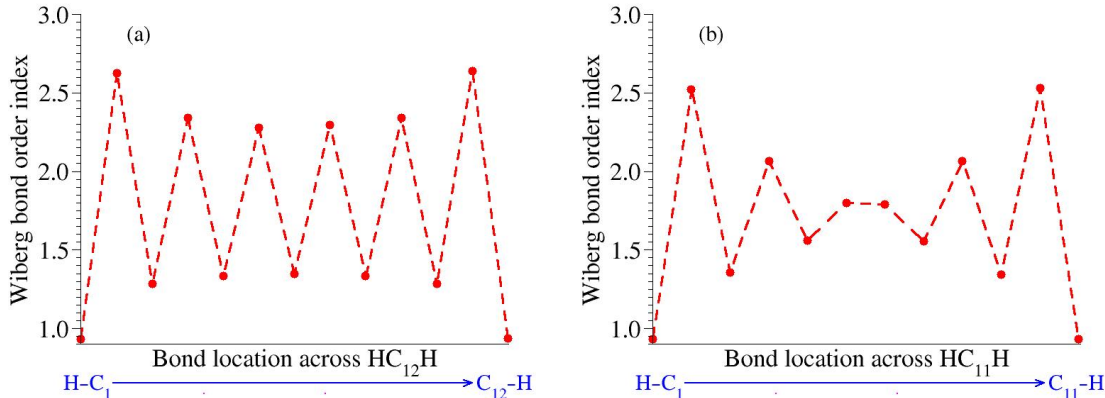


Figure 1: Wiberg bond order indices for HC_nH chains: (a) singlet HC_{12}H and (b) triplet HC_{11}H . The coordinates of these molecules at the corresponding energy minima as well as the HOMO spatial distributions are presented in Tables S7 and S6, and in Figures S2 and S1, respectively.

Table 1, which collects our results for the enthalpies of formation $\Delta_f H^0 = \Delta_f H^0(T)$ at zero $\Delta_f H^0_0$ and room temperature $\Delta_f H^0_{RT}$ ($T = 0\text{ K}$ and $T = 298.15\text{ K}$, respectively) and the related Figure 2a confirm this picture. As visible there, for the even members HC_{2k}H , the values $\Delta_f H^0|_S$ for singlet (S) isomers are smaller than the values $\Delta_f H^0|_T$ for triplet (T) isomers.

Table 1: Enthalpies of formation of linear HC_nH chains at zero and room temperature (subscript 0 and RT , respectively). Notice that for the even members HC_{2k}H the values for singlet (label S) are smaller than those for triplet (label T), while for the odd members HC_{2k+1}H the values for triplet are smaller than those for singlet.

Molec.	$\Delta_f H^0_0 _S$	$\Delta_f H^0_{RT} _S$	$\Delta_f H^0_0 _T$	$\Delta_f H^0_{RT} _T$
HC_2H	56.706	56.540	152.995	152.954
HC_3H	138.464	138.910	123.415	125.742
HC_4H	111.469	111.709	187.331	187.863
HC_5H	183.280	184.472	166.461	167.299
HC_6H^*	163.773	164.660	227.837	229.260
HC_7H	229.287	231.208	212.236	213.732
HC_8H	215.390	216.935	270.313	272.668
HC_9H	275.106	277.356	259.606	261.482
HC_{10}H	266.706	268.921	314.956	317.451
HC_{11}H	322.336	325.149	307.943	310.455
HC_{12}H	317.923	320.797	360.526	363.516

* Longest chain of this family astronomically observed.⁴²

Table 2: Adiabatic (Δ_{adiab}) and vertical ($\Delta_{S,T}$) values of the singlet-triplet energy separation (in eV) for HC_nH chains obtained within the methods indicated in the second column. The two vertical values shown here correspond to the optimized singlet (Δ_S) and triplet (Δ_T) geometries. Notice that the sign of Δ indicates that the most stable isomers are singlets for even members ($\Delta > 0$, HC_{2k}H) and triplets for odd members ($\Delta < 0$, HC_{2k+1}H). Corrections due to zero-point motion (label *corr*) were deduced within the DFT/B3LYP approach; see the last paragraph of Section 2. The almost equal values $\Delta_S \approx \Delta_T$ for larger odd-members (HC_nH , $n = 7, 9, 11$) indicate that the singlet and triplet geometries are similar ($\mathbf{R}_S \approx \mathbf{R}_T$, cf. Equation (2)).

Molec.	Method	Δ_{adiab}	Δ_S	Δ_T
HC_2H	B3LYP	4.269	5.739	2.285
HC_2H	B3LYP (corr)	4.176	5.645	2.191
HC_3H	B3LYP	-0.571	-0.044	-1.097
HC_3H	B3LYP (corr)	-0.653	-0.125	-1.179
HC_4H	B3LYP	3.410	4.532	1.856
HC_4H	B3LYP (corr)	3.290	4.411	1.735
HC_5H	B3LYP	-0.740	-0.376	-0.861
HC_5H	B3LYP (corr)	-0.729	-0.366	-0.850
HC_6H	B3LYP	2.930	3.579	1.809
HC_6H	B3LYP (corr)	2.778	3.427	1.657
HC_7H	B3LYP	-0.730	-0.729	-0.730
HC_7H	B3LYP (corr)	-0.740	-0.739	-0.740
HC_7H	CCSD	-0.885	-0.880	-0.881
HC_7H	CCSD(T)	-0.827	-0.820	-0.822
HC_8H	B3LYP	2.552	3.004	1.895
HC_8H	B3LYP (corr)	2.382	2.834	1.725
HC_8H	CCSD	3.403	3.776	2.455
HC_8H	CCSD(T)	3.211	3.693	2.529
HC_9H	B3LYP	-0.645	-0.647	-0.648
HC_9H	B3LYP (corr)	-0.672	-0.674	-0.675
HC_9H	CCSD	-0.823	-0.820	-0.821
HC_9H	CCSD(T)	-0.759	-0.754	-0.755
HC_{10}H	B3LYP	2.210	2.628	1.804
HC_{10}H	B3LYP (corr)	2.092	2.510	1.686
HC_{10}H	CCSD	3.137	2.997	2.378
HC_{10}H	CCSD(T)	2.928	2.902	2.426
HC_{11}H	B3LYP	-0.592	-0.591	-0.592
HC_{11}H	B3LYP (corr)	-0.624	-0.624	-0.625
HC_{11}H	CCSD	-0.787	-0.781	-0.783
HC_{11}H	CCSD(T)	-0.724	-0.716	-0.717
HC_{12}H	B3LYP	1.960	2.365	1.565
HC_{12}H	B3LYP (corr)	1.847	2.253	1.453
HC_{12}H	CCSD	2.981	3.241	2.151
HC_{12}H	CCSD(T)	2.721	3.109	2.185

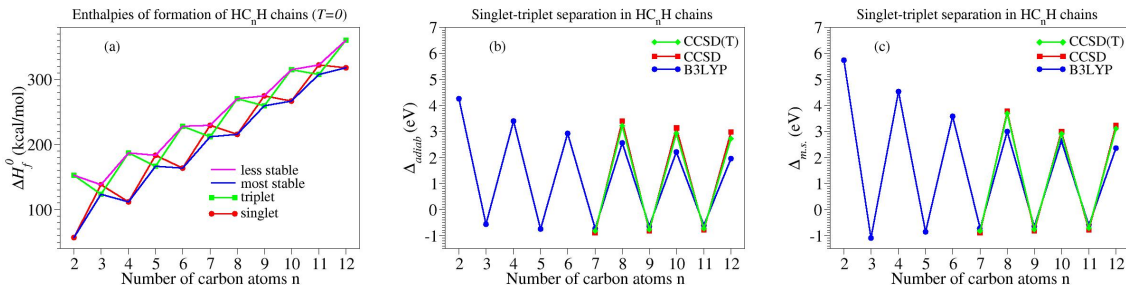


Figure 2: Results for HC_nH chains. (a) Enthalpies of formation for singlet and triplet chain isomers. (b) Adiabatic singlet-triplet separation energy Δ_{adiab} . (c) Vertical singlet-triplet separation at the geometry of the most stable state $\Delta_{m.s.}$ (namely, singlet for even members and triplet for odd members, *cf.* Equation (3)). Lines are guide to the eye. The numerical values underlying this figure are presented in Tables 1 and 2.

The alternation between single and triple bonds is incompatible with the standard rules of valence for the odd members species HC_{2k+1}H . Forms that could come into question here are either of polyne- (acetylenic)-type (*e.g.*, $\text{H}-\text{C}\equiv\text{C}-\dots\equiv\text{C}-\ddot{\text{C}}-\text{H}$) or of cumulene type (*e.g.*, $\text{H}-\dot{\text{C}}=\text{C}=\dots=\text{C}=\dot{\text{C}}-\text{H}$). As illustrated by a specific example, namely the HC_{11}H chain depicted in Figure 1b, calculations confirm the cumulene structure. By inspecting the enthalpies of formation (Table 1 and Figure 2a), one can see that the triplet state rather than the singlet state is the most stable form of the odd members of this family.

Above, we described the stability of the two subclasses (HC_{2k+1}H and HC_{2k}H) in a picture based on thermochemistry, which may not be the most adequate for systems of interest for astrochemistry, where single-molecule kinetic effects may prevail. Therefore, as a counterpart of this thermochemical analysis, in Table 2 and Figure 2b and c we also report results for the singlet-triplet separation energies Δ computed as differences between the corresponding total electronic energies of a molecule (*cf.* Section 2). The negative values ($\Delta \equiv \mathcal{E}_T - \mathcal{E}_S < 0$) for odd members indicate that the triplet state rather than the singlet state is preferably energetically for the odd members of this family, while the opposite ($\Delta > 0$) holds for even members, for which the singlet isomers are the most stable.

3.2 HC_nN Homologous Series

Let us next consider the related HC_nN family.

Out of the various carbon-based homologous series, this is probably the most numerous family investigated in different contexts in the past.^{9,11,12,18,43–46} In this case, it is the odd-member ($n = 2k + 1$) subclass HC_{2k+1}N ($k = 1, 2, \dots$) H–C $\equiv \dots$ –C \equiv N wherein the standard valence rules allow a singlet-triplet alternation of the carbon-carbon bonds along the chain. This is illustrated by the case of the HC₉N chain in Figure 3a. Calculations confirm that the electronic ground state of this HC_{2k+1}N cyanopolyne structure is of “normal” type, *i.e.*, a singlet state. Indeed, the corresponding enthalpies of formation for singlet are lower than for triplet ($\Delta_f H_0^0|_S < \Delta_f H_0^0|_T$), and the values of the singlet-triplet energy separation are positive ($\Delta > 0$); see Tables 3 and 4, and Figure 4.

Calculations for even members HC_{2k}N show that, out of the two possible forms — namely, of polyne type, *e.g.*, H– $\ddot{\text{C}}$ –C $\equiv \dots$ –C \equiv C–C \equiv N or of cumulene type, *e.g.*, H–C \equiv C– $\dot{\text{C}}$ =C= \dots =C= $\dot{\text{C}}$ –C \equiv — it is the latter that occurs. To exemplify, in Figure 3b we depict the case of the HC₈N chain. Our results for the even members HC_{2k}N are presented in Tables 3 and 4, and Figure 4a. They demonstrate an “anomalous” behavior; the triplet state is more stable than the singlet state. The enthalpies of formation (Table 3 and Figure 4a) for triplet are lower than for singlet, the singlet-triplet separation energies (Table 4 and Figure 4b and c) are negative.

To sum up, the electronic ground state for even members HC_{2k}N is a triplet state, which is in contrast with the singlet electronic ground state of the odd members HC_{2k+1}N.

3.3 C_nS Homologous Series

In the examples presented in Sections 3.1 and 3.2, we have seen that, in contrast to (either even or odd) members of the same homologous series consisting of “normal” (nonradical) species (HC_{2k}H and HC_{2k+1}N, respectively), “non-normal” (diradical)⁴¹ carbon chains wherein the alternation of single and triple carbon-carbon bonds (HC_{2k+1}H and HC_{2k}N,

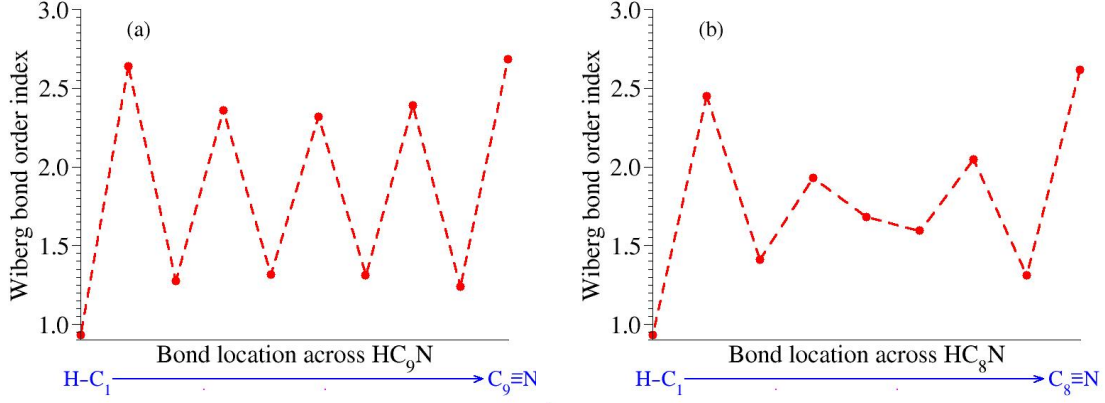


Figure 3: Wiberg bond order indices for HC_nN chains: (a) singlet HC_9N and (b) triplet HC_8N . The coordinates of these molecules at the corresponding energy minima as well as the HOMO spatial distributions are presented in Tables S11 and S10, and in Figures S4 and S3, respectively.

Table 3: Enthalpies of formation of linear HC_nN chains at zero and room temperature (subscript 0 and RT , respectively). Notice that for the odd members HC_{2k+1}N the values for singlet (label S) are smaller than those for triplet (label T), while for the even members HC_{2k}N the values for triplet are smaller than those for singlet.

Molec.	$\Delta_f H_0^0$	$\Delta_f H_{RT}^0 _S$	$\Delta_f H_0^0$	$\Delta_f H_{RT}^0 _T$
HCN	30.479	30.369	135.813	135.906
HC_2N	122.292	122.567	106.606	107.014
HC_3N	88.613	88.933	174.805	175.320
HC_4N	164.202	165.109	146.902	147.703
HC_5N	141.802	142.735	205.424	206.859
HC_6N	209.099	210.827	191.840	193.150
HC_7N	193.670	195.288	246.645	248.688
HC_8N	254.993	257.248	238.960	241.102
HC_9N	245.201	247.476	290.266	292.834
HC_{10}N	301.872	304.711	287.203	289.986
HC_{11}N^*	296.620	299.539	336.070	339.228
HC_{12}N	349.939	353.385	336.219	339.636

* Longest carbon chain ever claimed in astronomical observations¹⁸

Table 4: Adiabatic (Δ_{adiab}) and vertical ($\Delta_{S,T}$) values of the singlet-triplet energy separation (in eV) for HC_nN chains obtained within the methods indicated in the second column. The two vertical values shown here correspond to the optimized singlet (Δ_S) and triplet (Δ_T) geometries. Notice that the sign of Δ indicates that the most stable isomers are singlets for odd members ($\Delta > 0$, HC_{2k+1}N) and triplets for even members ($\Delta < 0$, HC_{2k}N). Corrections due to zero-point motion (label *corr*) were deduced within the DFT/B3LYP approach; see the last paragraph of Section 2. The almost equal values $\Delta_S \approx \Delta_T$ for larger even-members (HC_nN , $n = 8, 10, 12$) indicate that the singlet and triplet geometries are similar ($\mathbf{R}_S \approx \mathbf{R}_T$, *cf.* Equation (2)).

Molec.	Method	Δ_{adiab}	Δ_S	Δ_T
HCN	B3LYP	4.670	7.438	3.141
HCN	B3LYP (corr)	4.568	7.336	3.039
HC ₂ N	B3LYP	-0.658	-0.223	-1.116
HC ₂ N	B3LYP (corr)	-0.680	-0.245	-1.138
HC ₃ N	B3LYP	3.845	4.961	2.318
HC ₃ N	B3LYP (corr)	3.738	4.854	2.210
HC ₄ N	B3LYP	-0.731	-0.326	-0.925
HC ₄ N	B3LYP (corr)	-0.750	-0.345	-0.944
HC ₅ N	B3LYP	2.898	3.456	2.120
HC ₅ N	B3LYP (corr)	2.759	3.317	1.981
HC ₆ N	B3LYP	-0.753	-0.601	-0.766
HC ₆ N	B3LYP (corr)	-0.748	-0.597	-0.762
HC ₇ N	B3LYP	2.407	2.865	1.960
HC ₇ N	B3LYP (corr)	2.297	2.755	1.849
HC ₈ N	B3LYP	-0.670	-0.669	-0.670
HC ₈ N	B3LYP (corr)	-0.695	-0.695	-0.696
HC ₈ N	CCSD	-0.837	-0.832	-0.833
HC ₈ N	CCSD(T)	-0.774	-0.766	-0.768
HC ₉ N	B3LYP	2.058	2.703	1.640
HC ₉ N	B3LYP (corr)	1.954	2.599	1.536
HC ₉ N	CCSD	3.194	3.514	2.433
HC ₉ N	CCSD(T)	2.999	3.430	2.494
HC ₁₀ N	B3LYP	-0.607	-0.606	-0.607
HC ₁₀ N	B3LYP (corr)	-0.636	-0.636	-0.637
HC ₁₀ N	CCSD	-0.807	-0.787	-0.789
HC ₁₀ N	CCSD(T)	-0.728	-0.722	-0.723
HC ₁₁ N	B3LYP	1.815	2.413	1.411
HC ₁₁ N	B3LYP (corr)	1.711	2.309	1.307
HC ₁₁ N	CCSD	2.551	2.839	1.721
HC ₁₁ N	CCSD(T)	2.350	2.742	1.813
HC ₁₂ N	B3LYP	-0.563	-0.562	-0.563
HC ₁₂ N	B3LYP (corr)	-0.595	-0.594	-0.595

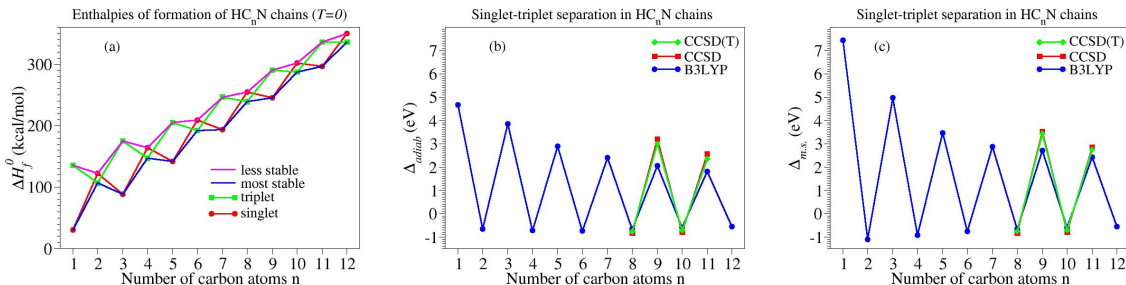


Figure 4: Results for HC_nN chains. (a) Enthalpies of formation for singlet and triplet chain isomers. (b) Adiabatic singlet-triplet separation energy Δ_{adiab} . (c) Vertical singlet-triplet separation at the geometry of the most stable state $\Delta_{m.s.}$ (namely, singlet for odd members and triplet for even members, *cf.* Equation (3)). Lines are guide to the eye. The numerical values underlying this figure are presented in Tables 3 and 4.

respectively) is incompatible with standard valence considerations possess triplet electronic ground states. Does this diradical character necessarily make carbon-based chains adopting triplet ground states?

To answer this question, it is meaningful to investigate carbon-based chains wherein both even and odd members of the molecular series possess two electrons that cannot be involved in covalent bonds. Linear carbon chains terminated with a sulfur atom C_nS (S=C=...=C•), which we next consider and were also reported in astronomical observations (*e.g.*, refs. 13, 47,48), belong to this category.

As exemplified with the aid of the cases of the C₆S and C₇S chains depicted in Figure 5, calculations confirm the cumulene-type structure both for even and odd members. This result is not surprising; it can be expected based on chemical intuition. However, what is nontrivial is the fact that the state corresponding to the lowest electronic energy is found to be a singlet state for odd members C_{2k+1}S, while for even members C_{2k}S the lowest state is a triplet. Indeed, the results of our calculations presented in Table 5 and Figure 6a show that the lower enthalpies of formation correspond to singlet isomers for odd members C_{2k+1}S and to triplet isomers for even members C_{2k}S. Alternatively rephrased, the negative values of the singlet-triplet energy splitting Δ demonstrate that the triplet state is the most stable for even members (C_{2k}S), in contrast to the odd members (C_{2k+1}S) for which the most stable

is a singlet, as expressed by the positive Δ -values (*cf.* Table 6 and Figure 6b and c).

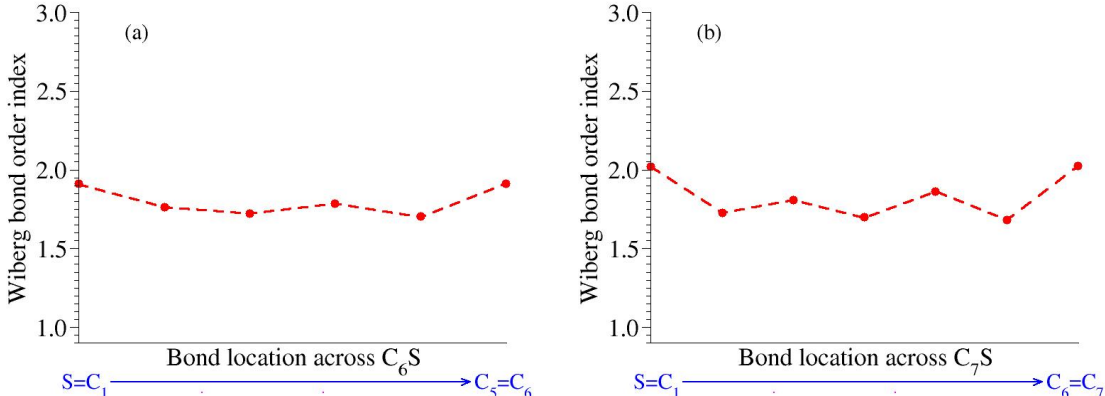


Figure 5: Wiberg bond order indices for C_nS chains: (a) triplet C_6S and (b) singlet C_7S . The coordinates of these molecules at the corresponding energy minima as well as the HOMO spatial distributions are presented in Tables S14 and S15 and in Figures S5 and S6, respectively.

Table 5: Enthalpies of formation of linear C_nS chains at zero and room temperature (subscript 0 and RT , respectively). Notice that for the odd members $C_{2k+1}S$ the values for singlet (label S) are smaller than those for triplet (label T), while for the even members $C_{2k}S$ the values for triplet are smaller than those for singlet.

Molec.	$\Delta_f H_0^0$	$\Delta_f H_{RT}^0 _S$	$\Delta_f H_0^0$	$\Delta_f H_{RT}^0 _T$
CS	70.934	69.634	146.830	147.617
C_2S	162.418	163.565	145.630	146.834
C_3S	135.505	136.805	190.378	191.944
C_4S	196.846	198.489	182.693	184.308
C_5S *	191.231	193.097	232.108	234.229
C_6S	243.319	245.553	232.214	234.417
C_7S	245.291	247.800	276.777	279.455

* Longest chain of this family astronomically observed^{47,48}

3.4 C_nO Homologous Series

Let us next consider linear carbon chains terminated with an oxygen atom (C_nO). Similar to C_nS , C_nO chains also possess two electrons that cannot be involved in covalent bonds. Such chains were also reported in astronomical observations.¹³

Calculations confirm again the cumulene-type structure of the ground state $O=C=\dots=C\cdot$ irrespective whether the number of carbon atoms is even or odd. Figure 7 illustrates this

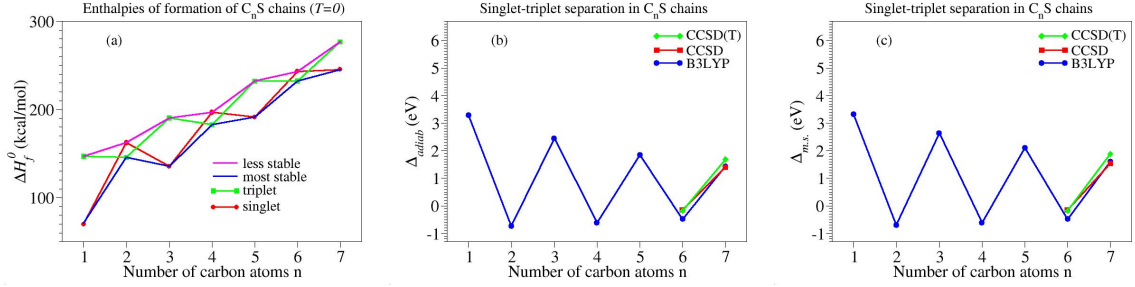


Figure 6: Results for $C_n S$ chains. (a) Enthalpies of formation for singlet and triplet chain isomers. (b) Adiabatic singlet-triplet separation energy Δ_{adiab} . (c) Vertical singlet-triplet separation at the geometry of the most stable state $\Delta_{m.s.}$ (namely, singlet for odd members and triplet for even members, *cf.* Equation (3)). Lines are guide to the eye. The numerical values underlying this figure are presented in Tables 5 and 6.

Table 6: Adiabatic (Δ_{adiab}) and vertical ($\Delta_{S,T}$) values of the singlet-triplet energy separation (in eV) for $C_n S$ chains obtained within the methods indicated in the second column. The two vertical values shown here correspond to the optimized singlet (Δ_S) and triplet (Δ_T) geometries. Notice that the sign of Δ indicates that the most stable isomers are singlets for odd members ($\Delta > 0$, $C_{2k+1} S$) and triplets for even members ($\Delta < 0$, $C_{2k} S$). Corrections due to zero-point motion (label *corr*) were deduced within the DFT/B3LYP approach; see the last paragraph of Section 2.

Molec.	Method	Δ_{adiab}	Δ_S	Δ_T
CS	B3LYP	3.302	3.330	3.268
CS	B3LYP (corr)	3.291	3.320	3.258
C_2S	B3LYP	-0.723	-0.691	-0.700
C_2S	B3LYP (corr)	-0.728	-0.696	-0.705
C_3S	B3LYP	2.447	2.644	1.412
C_3S	B3LYP (corr)	2.380	2.576	1.345
C_4S	B3LYP	-0.613	-0.613	-0.614
C_4S	B3LYP (corr)	-0.614	-0.613	-0.614
C_5S	B3LYP	1.848	2.107	1.787
C_5S	B3LYP (corr)	1.773	2.031	1.711
C_6S	B3LYP	-0.480	-0.480	-0.481
C_6S	B3LYP (corr)	-0.482	-0.481	-0.482
C_6S	CCSD	-0.140	-0.140	-0.141
C_6S	CCSD(T)	-0.175	-0.177	-0.177
C_7S	B3LYP	1.442	1.615	1.407
C_7S	B3LYP (corr)	1.365	1.539	1.331
C_7S	CCSD	1.406	1.544	1.363
C_7S	CCSD(T)	1.687	1.882	1.691

fact for the specific case of C_6O and C_7O chains. Inspection reveals only slight differences between this figure and Figure 5, which refers to the isoelectronic C_6S and C_7S chains. The slightly broader range of the bond order index variation in Figure 7 as compared to Figure 5 can be attributed to the oxygen electronegativity ($\chi_O^{Pauling} = 3.44$, $\chi_O^{Allen} = 3.610$), which is larger than the sulfur electronegativity ($\chi_S^{Pauling} = 2.58$, $\chi_S^{Allen} = 2.589$). Calculations also

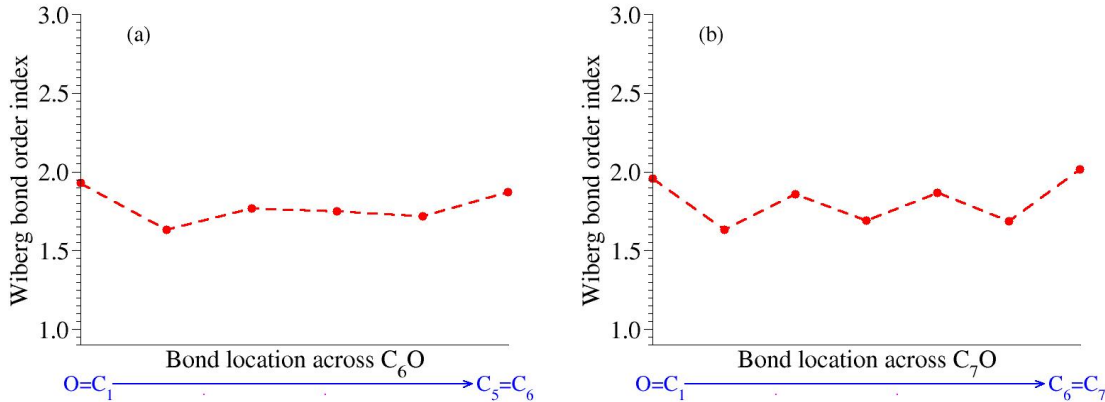


Figure 7: Wiberg bond order indices for C_nO chains: (a) triplet C_6O and (b) singlet C_7O . The coordinates of these molecules at the corresponding energy minima as well as the HOMO spatial distributions are presented in Tables S18 and S19 and in Figures S7 and S8, respectively.

confirm the alternation of the singlet and triplet states of the C_nO chains with increasing number of carbon atoms found for the isoelectronic C_nS chains reported in Section 3.3. The values of the enthalpies of formations (Table 7 and Figure 8a) and the singlet-triplet separations (Table 8 and Figures 8b and 8c) demonstrate that, for even members ($C_{2k}O$), the triplet state is more stable than the singlet state while the opposite holds true for the odd members ($C_{2k+1}O$).

3.5 OC_nO Homologous Series

Out of the chains investigated in Sections 3.1 and 3.2, all diradical species $HC_{2k+1}H$ and $HC_{2k}N$ turned out to possess triplet ground states. The results of Sections 3.3 and 3.4 indicated that the diradical character of a carbon chain does not automatically imply that

Table 7: Enthalpies of formation of linear C_nO chains at zero and room temperature (subscript 0 and RT , respectively). Notice that for the odd members $C_{2k+1}O$ the values for singlet (label S) are smaller than those for triplet (label T), while for the even members $C_{2k}O$ the values for triplet are smaller than those for singlet.

Molec.	$\Delta_f H_0^0$	$\Delta_f H_{RT}^0 _S$	$\Delta_f H_0^0$	$\Delta_f H_{RT}^0 _T$
CO	-24.140	-23.356	110.602	111.387
C_2O	110.227	111.332	85.497	86.550
C_3O *	76.170	77.389	143.236	144.734
C_4O	149.118	150.669	133.039	134.532
C_5O	135.765	137.516	186.814	188.994
C_6O	193.343	195.458	181.261	183.327
C_7O	190.940	193.324	228.914	231.450

* Longest chain of this family astronomically observed¹³

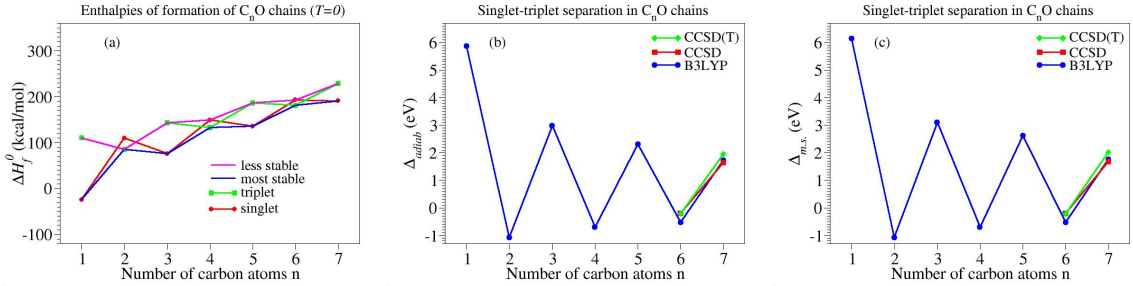


Figure 8: Results for C_nO chains. (a) Enthalpies of formation for singlet and triplet chain isomers. (b) Adiabatic singlet-triplet separation energy Δ_{adiab} . (c) Vertical singlet-triplet separation at the geometry of the most stable state $\Delta_{m.s.}$ (namely, singlet for odd members and triplet for even members, *cf.* Equation (3)). Lines are guide to the eye. The numerical values underlying this figure are presented in Tables 7 and 8.

Table 8: Adiabatic (Δ_{adiab}) and vertical ($\Delta_{S,T}$) values of the singlet-triplet energy separation (in eV) for C_nO chains obtained within the methods indicated in the second column. The two vertical values shown here correspond to the optimized singlet (Δ_S) and triplet (Δ_T) geometries. Notice that the sign of Δ indicates that the most stable isomers are singlets for odd members ($\Delta > 0$, $C_{2k+1}O$) and triplets for even members ($\Delta < 0$, $C_{2k}O$). Corrections due to zero-point motion (label *corr*) were deduced within the DFT/B3LYP approach; see the last paragraph of Section 2.

Molec.	Method	Δ_{adiab}	Δ_S	Δ_T
CO	B3LYP	5.869	6.148	5.572
CO	B3LYP (corr)	5.843	6.122	5.545
C ₂ O	B3LYP	-1.078	-1.063	-1.072
C ₂ O	B3LYP (corr)	-1.072	-1.058	-1.067
C ₃ O	B3LYP	2.988	3.104	2.143
C ₃ O	B3LYP (corr)	2.908	3.024	2.063
C ₄ O	B3LYP	-0.698	-0.698	-0.699
C ₄ O	B3LYP (corr)	-0.697	-0.697	-0.698
C ₅ O	B3LYP	2.314	2.626	2.221
C ₅ O	B3LYP (corr)	2.214	2.525	2.121
C ₆ O	B3LYP	-0.523	-0.523	-0.524
C ₆ O	B3LYP (corr)	-0.524	-0.523	-0.524
C ₆ O	CCSD	-0.194	-0.193	-0.194
C ₆ O	CCSD(T)	-0.217	-0.219	-0.220
C ₇ O	B3LYP	1.725	1.761	1.684
C ₇ O	B3LYP (corr)	1.647	1.683	1.606
C ₇ O	CCSD	1.645	1.681	1.595
C ₇ O	CCSD(T)	1.956	2.025	1.962

the most stable state is a triplet. Although all C_nS and C_nO chains are diradical species, only the $C_{2k}S$ and $C_{2k}O$ chains considered have triplet ground states; the $C_{2k+1}S$ and $C_{2k+1}O$ chains possess singlet ground states.

Conversely, because the most stable isomers of the “normal” (nonradical) chains $HC_{2k}H$ and $HC_{2k+1}N$ examined in Sections 3.1 and 3.2 were found to be a singlet state, one may next ask whether all nonradical carbon-based chains possess singlet ground states. In order to inquire this possibility, we will next consider carbon chains having oxygen atoms attached at the both ends (OC_nO).

Irrespective whether the number of carbon atoms is even or odd, the cumulene-type structure $O=C=\dots=C=O$ characterized by successive double bonds along the chain ensures that all valence electrons are involved in chemical (double) bonds. Results of calculations confirming this behavior are depicted in Figure 9.

Still, in spite of the fact that both even and odd members of this family are “normal”

molecules with a similar (cumulene-type) structure, their most stable form is not necessarily a singlet state. As seen in Table 9 and Figure 10a, only odd members (OC_{2k+1}O) have enthalpies of formation for singlet lower than for triplet. However, for even members (OC_{2k}O), triplet isomers possess enthalpies of formation lower than for singlets. The fact that the most stable form is a singlet state for odd members but a triplet for even members can alternatively be seen by inspecting the single-triplet energy separations Δ (*cf.* Table 10, and Figure 10b and c), which are positive for OC_{2k+1}O but negative for OC_{2k}O .

To conclude this subsection, carbon-based chains can have a triplet ground state notwithstanding the fact that the corresponding species have always “normal” (nonradical) character. Parenthetically, one can still note that, in carbon chains, a triplet state yields an overall enforcement of the cumulenic character even in species (*e.g.*, HC_{12}H , Figure S11 of the SI) where the most stable isomer is of singlet polyynes type compatible with the standard rules of valence.

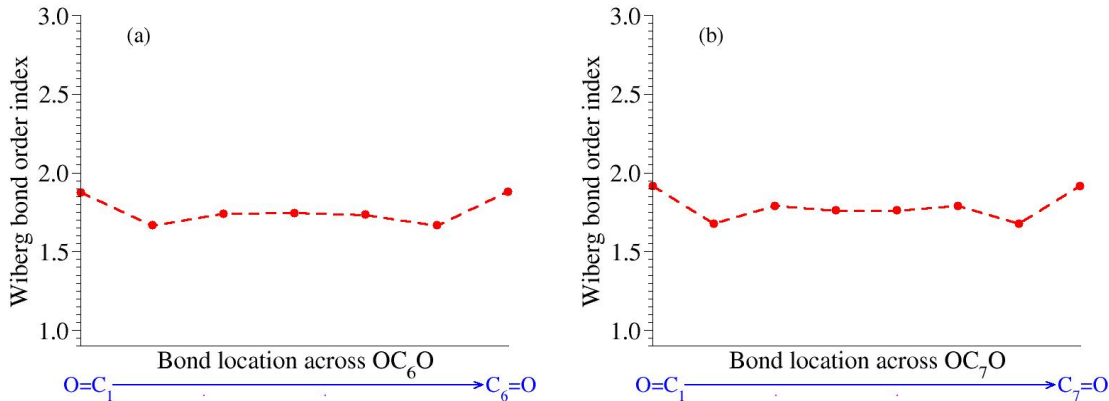


Figure 9: Wiberg bond order indices for OC_nO chains: (a) triplet OC_6O and (b) singlet OC_7O . The coordinates of these molecules at the corresponding energy minima as well as the HOMO spatial distributions are presented in Tables S22 and S23 and in Figures S9 and S10 respectively.

Table 9: Enthalpies of formation of linear OC_nO chains at zero and room temperature (subscript 0 and RT , respectively). Notice that for the odd members OC_{2k+1}O the values for singlet (label S) are smaller than those for triplet (label T), while for the even members OC_{2k}O the values for triplet are smaller than those for singlet. (Values for singlet OC_2O are missing; calculations for geometry optimization invariably yielded two spatially separated CO dimers.)

Molec.	$\Delta_f H_0^0$	$\Delta_f H_{RT}^0 _S$	$\Delta_f H_0^0$	$\Delta_f H_{RT}^0 _T$
OCO	-94.430	-94.529	16.393	16.655
OC_2O	—	—	-7.416	-6.796
OC_3O	-29.465	-26.888	43.260	44.194
OC_4O	44.030	45.323	31.070	32.001
OC_5O	29.782	30.933	84.659	86.351
OC_6O	88.330	90.169	78.024	79.532
OC_7O	85.409	87.231	126.150	128.203

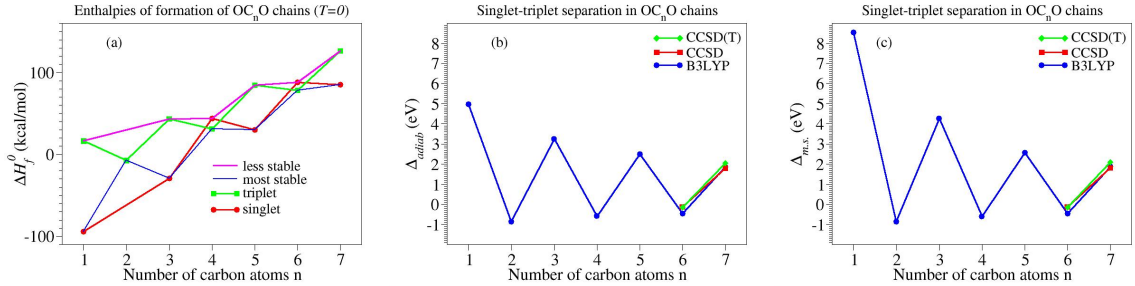


Figure 10: Results for OC_nO chains. (a) Enthalpies of formation for singlet and triplet chain isomers. (b) Adiabatic singlet-triplet separation energy Δ_{adiab} . (c) Vertical singlet-triplet separation at the geometry of the most stable state Δ_{ms} . (namely, singlet for odd members and triplet for even members, *cf.* Equation (3)). Lines are guide to the eye. The numerical values underlying this figure are presented in Tables 9 and 10. (Values for singlet OC_2O are missing; calculations for geometry optimization invariably yielded two spatially separated CO dimers.)

Table 10: Adiabatic (Δ_{adiab}) and vertical ($\Delta_{S,T}$) values of the singlet-triplet energy separation (in eV) for $O C_n O$ chains obtained within the methods indicated in the second column. The two vertical values shown here correspond to the optimized singlet (Δ_S) and triplet (Δ_T) geometries. Notice that the sign of Δ indicates that the most stable isomers are singlets for odd members ($\Delta > 0$, $OC_{2k+1}O$) and triplets for even members ($\Delta < 0$, $OC_{2k}O$). Corrections due to zero-point motion (label *corr*) were deduced within the DFT/B3LYP approach; see the last paragraph of Section 2.

Molec.	Method	Δ_{adiab}	Δ_S	Δ_T
OCO	B3LYP	4.977	8.549	3.001
OCO	B3LYP (corr)	4.806	8.378	2.830
OC ₂ O	B3LYP	—	—	-0.856
OC ₂ O	B3LYP (corr)	—	—	—
OC ₃ O	B3LYP	3.247	4.273	1.130
OC ₃ O	B3LYP (corr)	3.154	4.179	1.037
OC ₄ O	B3LYP	-0.583	-0.583	-0.584
OC ₄ O	B3LYP (corr)	-0.562	-0.562	-0.562
OC ₅ O	B3LYP	2.491	2.570	1.724
OC ₅ O	B3LYP (corr)	2.380	2.459	1.612
OC ₆ O	B3LYP	-0.447	-0.447	-0.447
OC ₆ O	B3LYP (corr)	-0.447	-0.447	-0.448
OC ₆ O	CCSD	-0.124	-0.126	-0.126
OC ₆ O	CCSD(T)	-0.142	-0.145	-0.145
OC ₇ O	B3LYP	1.855	1.873	1.836
OC ₇ O	B3LYP (corr)	1.767	1.786	1.748
OC ₇ O	CCSD	1.802	1.822	1.778
OC ₇ O	CCSD(T)	2.057	2.107	2.072

3.6 Infrared and UV-Visible Absorption of Carbon Chains in Singlet and Triplet States

One of the main aims of this paper is to emphasize that the lowest electronic state of carbon-based chains of interest for astrochemistry systematically switches back and forth between singlet and triplet as the carbon chain length increases. A detailed analysis of the differences between properties of the lowest singlet and triplet states for each carbon-based chain of astrochemical interest is certainly important, *e.g.*, for adequately processing data acquired (or to be acquired) in astronomical observations. This analysis is out of the scope of the present paper and will be deferred to a forthcoming publication.

Certainly, the nature of the ground state (*i.e.*, singlet *vs* triplet) can have a pronounced impact on various observable molecular properties. While important differences between properties of singlet and triplet states of various molecular species would not be surprising in general, the specific example presented below reveals that the impact can be significant

even in situations less expected.

For illustration, let us consider HC_{11}H chains. By inspection the HOMO spatial distributions of HC_{11}H chains (*cf.* Figure S1) one can conclude that the differences between the singlet and triplet states are rather minor. Nevertheless, the infrared spectra presented in Figure 11 (calculated within the harmonic approximation) reveal significant differences between the singlet and triplet HC_{11}H isomers.

Less surprisingly, calculations showed that the spin multiplicity has little impact on the high frequency strong peak depicted in Figure 11 due to the stretching mode of the C–H bonds with pronounced s-character; the corresponding frequency values ($\nu_{\text{C-H}}^{\text{S}} = 3462.46 \text{ cm}^{-1}$ and $\nu_{\text{C-H}}^{\text{T}} = 3461.93 \text{ cm}^{-1}$) are identical within the numerical accuracy. However, as visible in Figure 11, differences between the singlet and triplet HC_{11}H infrared spectra significant especially in the spectral range $\sim 400 - 800 \text{ cm}^{-1}$ characteristic for CCH bending modes. We referred above to vibrational properties because infrared (vibrational) spectroscopy is an important tool for detecting symmetric molecules like HC_{11}H ; given the fact that their dipole moment vanishes, rotational spectroscopy cannot be utilized in such cases. Another example revealing the impact of the nature of the ground state on the infrared

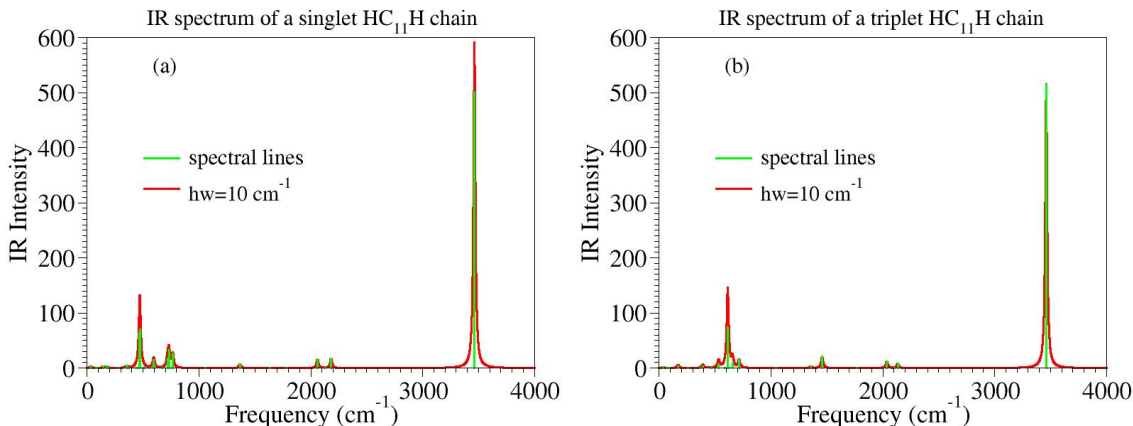


Figure 11: Infrared spectra of (a) singlet and (b) triplet HC_{11}H chains. The solid red lines were deduced by convoluting the spectral lines (depicted in green) computed within a DFT/B3LYP/6-311++g(3df, 3pd) approach by using Lorentzian distributions whose halfwidth (hw) is indicated in the legend.

spectra is presented in the SI; see Figures S12a and S12b.

In addition to the significant impact on the vibrational transitions underlying the differences between the singlet and triplet infrared spectra of Figures 11a and 11b, we can also mention a similar effect on the UV-visible absorption. To exemplify, our TD-DFT/CAM-B3LYP/6-311++g(3df, 3pd) calculations yielded a value $\varepsilon_T = 2.614\text{ eV}$ (474 nm) for the lowest $A^3\Sigma^- - X^3\Sigma^-$ electronic transition. Similar calculations done for the lowest electronic transition of the singlet HC_{11}H found a significantly different value of $\varepsilon_S = 2.303\text{ eV}$ (538 nm).

One should still note here that estimates based on the methods utilized above may not be sufficiently accurate to be directly compared with measured data.

Unfortunately, *ab initio* (e.g., CC-)methods to compute vibrational properties for such large and open shell molecular species, which can be employed to smaller closed-shell chains,⁴⁰ are currently prohibitive. Still, we believe that the significant differences between Figure 11a and b (and between Figure S12a and b of the SI) represent a convincing argument that experiments — which the present theoretical study hopes to motivate — can discriminate between the singlet and triplet HC_{11}H (and HC_{12}H) chains.

Likewise, the above TD-DFT-based $\varepsilon_{S,T}$ -values may not be accurate enough for quantitative purposes. Still, given the fact that *ab initio* calculations for excited states of open-shell systems at such large molecular sizes represents a formidable challenge for theory, the magnitude of the difference $\varepsilon_T - \varepsilon_S$ found above should be sufficiently significant to encourage companion experimental efforts.

3.7 A *Sui Generis* Even-Odd Effect that Confounds Straightforward Chemical Intuition

It is known that successive addition of repeat units to homologous classes of systems may result in properties periodically switching back and forth in a manner similar to that depicted in our Figures 2, 4, 6, 8, and 10. Examples of this kind include, e.g., the case of aromatic $4n+2$ (Hückel) and $4n$ (anti-Hückel) cyclic polyenes (annulenes) dating back to the early days of

quantum mechanics^{32-35,49} or their more recent counterpart in mesoscopic and quantum dot rings²⁸⁻³¹ as well as a variety of even-odd effects in multilayers,²⁶ self-assembled monolayers,²⁷ molecular electronic devices,^{2,3} or atomic nuclei.

Compared to those and all other cases of which we are aware, the even-odd effect reported previously²⁵ and extensively analyzed in this paper for carbon-based chains of astrochemical interest is unique. This even-odd effect does not merely consist of an alternation of a certain (ground state) property upon size increasing. Rather, it is the very nature of the electronic ground state that switches back and forth between a singlet and triplet state. Specifically, we showed here that, depending on the chemical nature of the terminal heteroatom(s), the chain possesses a singlet ground state for a certain parity (*i.e.*, even or odd) of the number of carbon atoms, which switches to a triplet ground state for the other parity (odd or even, respectively) of this number.

It is worth emphasizing that the singlet-triplet alternation discussed above is a subtle effect that confounds straightforward intuition. We first considered (Sections 3.1 and 3.2) carbon chain families, wherein members of a certain parity are normal (closed-shell, non-radical) molecules having all valence electrons paired in chemical bonds between adjacent atoms while members of the opposite parity are diradicals. Chains of HC_nH and HC_nN (as well as NC_nN , a case not explicitly discussed because of its similarity with the first two) belonging to this category seemed to fit an intuitive rule of thumb (ground state of normal chains is a singlet, diradical chains have triplet ground states). In disagreement to that, subsequent examples examined revealed that not all diradical chains (C_nS , Section 3.3 and C_nO , Section 3.4) have a triplet ground state, while not all normal (nonradical) chains (OC_nO , Section 3.5) possess singlet ground states.

3.8 Remarks on Some Recent Studies on Carbon Chains Done in the Astrophysics/Astronomical Community

Without any intention to target the entire astrophysical/astrochemical community, we have to emphasize that our present findings disagree with some recent studies^{22–24} claiming that, for all carbon-based chains with an even number of electrons like those examined above singlet isomers are the most stable. Refuting that claim and drawing attention on the fact that triplet states deserve consideration in astrochemical context (*cf.* Section 3.10 below) was an important aim of conducting the extensive theoretical investigation presented in this paper.

To demonstrate that, even if not explicitly stated, ref. 22 tacitly admitted singlet electronic ground states, in Tables S1–S4 of the SI we present results reported in that work along with $\Delta_f H^0$ -estimates for both singlets and triplets based on the DFT/B3LYP/6-311++g(3df, 3pd) approach underlying Tables 1, 3, 7, 5, and 9. As visible from the inspection of Tables S1–S4, the $\Delta_f H^0$ -values of ref. 22 agree with our $\Delta_f H^0$ values obtained for the lowest singlet states. So, although not explicitly stated in ref. 22, the results presented there do refer to the singlet states. The small differences between $\Delta_f H^0$ -values of Tables 1, 3, 7, 5, and 9 and those of ref. 22 may reflect the slightly different methods utilized. These differences due to the different approaches are comparable to those between the B3LYP/6-311++g(3df, 3pd)-based values and the $\Delta_f H^0$ -estimates obtained by using the CBS-QB3 protocol as implemented in GAUSSIAN 16, which are also shown in Tables S1–S4 for comparison purposes.

3.9 Computational Issues

Important insight from a computational perspective can be gained from the comparison between the various estimates presented in Tables 2, 4, 6, 8, and 10.

First, the results presented there emphasize limitations of popular Delta-SCF⁵⁰ or Delta-

DFT^{51–53} methods to estimate the singlet-triplet energy separation. Properties like the singlet-triplet separation Δ examined above as well as other quantities, *e.g.*, ionization or electron attachment energies can be expressed as differences between pertaining total molecular energies. Similar to other cases,^{53–55} the comparison with state-of-the-art approaches based on coupled-cluster expansions (*cf.* Tables 2, 4, 6, 8, and 10) reveals differences of several tenth of electronvolt. Such differences are significantly larger than the accuracy needed for reliable astrochemical modeling or achieved in experiments.^{56,57}

More importantly, the differences between CCSD and CCSD(T) estimates appear to be unusually large. In “normal” cases, where electron correlations are “moderately” strong, quantities obtained within the CCSD(T) approach do not substantially differ from those based on the CCSD approach. The reason is that, within the CCSD(T) approach, triple excitations are only *perturbatively* treated on top of the single and double excitations embodied within the CCSD approach. Such a perturbative approach can be hardly justified in cases like those shown above for longer chains, where the differences between CCSD(T) and CCSD estimates amount to $\sim 0.3 - 0.4$ eV (*cf.* Tables 6, 8, and 10). This state of affairs calls for further clarification. Possible further developments in this direction include other theoretical treatments (*e.g.*, SAC-CI⁵⁸), CC approaches including higher order electron correlations (*e.g.*, CCSDT or CC3⁵⁹) or based on the (particularly suited for one-dimensional systems) density matrix renormalization group (DMRG).^{60–62}

3.10 Relevance for Astronomical Detectability

From an astrochemical perspective, the inspection of the results presented above unravels a striking correlation. Across the various families of linear carbon-chains presently considered, the members that were not identified in astronomical data are preponderantly those for which our present calculations predict a triplet ground state. Examples will be presented below in support of this assertion.

C₅S is the longest chain detected in space⁴⁷ from the C_nS family. However, the shorter C₄S chain was not reported so far. Still, the enthalpy of formation for the most stable C₄S chain (which is a *triplet*) is lower than that for the most stable (singlet) C₅S chain observed (*cf.* Table 5). On the contrary, the less stable singlet C₄S isomer has an enthalpy of formation higher than that of the singlet C₅S chain. So, it is not unexpected that it is more difficult to detect C₄S chains implicitly assuming that they are singlets than to detect (singlet) C₅S chains.

A similar situation is encountered in the HC_nH series. Out of the HC_nH family, HC₆H is the longest chain observed.⁴² Nevertheless, the shorter HC₅H chain was not detected in space so far. Its most stable (*triplet*) isomer is more stable than the most stable (singlet) HC₆H chain (*cf.* Table 1) although the singlet HC₅H chain is thermodynamically less stable than the singlet HC₆H chain.

Most notorious is the case of the HC_nN family. The even members HC₆N, HC₈N, and HC₁₀N were not observed in space; nevertheless, the next larger odd members HC₇N,¹¹ HC₉N,¹² and HC₁₁N¹⁸ were detected in astronomical data. The inspection of Table 3 reveals that, again, it is the most stable (*triplet*) isomer of the even members that is more stable than the most stable (singlet) isomer of the next larger isomer of the odd members. A *triplet* HC₆N chain is more stable thermodynamically than a singlet HC₇N chain, a *triplet* HC₈N chain is more stable than a singlet HC₉N chain, and a *triplet* HC₁₀N chain is more stable than a singlet HC₁₁N chain,^{45,63} although a *singlet* HC₆N chain is less stable thermodynamically than a singlet HC₇N chain, a *singlet* HC₈N chain is less stable than a singlet HC₉N chain, and a *singlet* HC₁₀N chain is less stable than a singlet HC₁₁N chain.

In all cases of the aforementioned type, ref. 22 arrived at an opposite conclusion on the thermodynamical in/stability across various chain families because of the incorrect (implicit²³) assumption that the most stable chains of species with an even number of electrons are always singlets.

In Introduction we mentioned that information on the presently considered carbon-based

chains are very scarce. Given this data scarcity, it may be tempting to resort to empirical interpolation/extrapolation schemes;²⁴ namely, to utilize available properties of molecular species of a certain homologous family to deduce unavailable properties of other molecular species, and use the latter in attempting to reveal their presence by processing the astronomical data. However, such a procedure will inherently fail. Properties of, *e.g.*, *triplet* HC₆N, HC₈N or HC₁₀N chains can by no means be obtained by interpolating/extrapolating properties of *singlet* HC₇N, HC₉N and HC₁₁N chains. The reason of this failure should be clear; we have seen that differences between the singlet and triplet isomers of a given carbon chain may be important even in situations where one can expect that they are less significant (*cf.* Section 3.6).

4 Summary

In this paper, we demonstrated that, in families of carbon-based chains, most stable members of one parity (even or odd) are singlets while most stable members of the opposite parity (odd or even) are triplets. This is a *sui generis* effect qualitatively different from other even-odd effects known from studies over decades in other areas.^{2,3,26–35}

From a more general perspective, the present paper aimed at bridging astronomy/astrophysics and physical/computational chemistry. The results reported here are most significant in the context of the observability in space. As elaborated in Section 3.10, we strongly believe that it is not coincidental that absent in the list of various homologous series detected in space are just carbon-based chains for which our calculations predict a triplet ground state. Emphasizing that most stable isomers of carbon-based chains of the type considered in our paper are not invariably singlets is important because this was incorrectly claimed in some recent studies done in the astronomical/astrophysical community.^{22,24} Prior to the present extensive study, a series of authors drew attention on the fact that triplet isomers of carbon-based chains are more stable than singlet isomers: HC_{2k+1}H,^{25,64} C_{2k},^{25,65} HC₄N,^{66–69} NC₅N,⁷⁰

C_{2k}O ,⁷¹ $\text{C}_{2,4}\text{S}$,⁷² and HC_6N .⁷³

Last but not least, from a computational perspective, the present results are important because they emphasize that electron correlations in carbon-based chains are unusually strong. The analysis of Section 3.9 indicated that the “standard gold” CCSD(T) quantum chemical approach may not be sufficiently accurate to quantify these strong electron correlations. This is an important challenge for the community of theoretical chemistry that deserves further consideration.

Acknowledgment

I thank Jochen Schirmer for stimulating discussions. Financial support for this research provided by the Deutsche Forschungsgemeinschaft (DFG grant BA 1799/3-1,2) and partial computational support by the State of Baden-Württemberg through bwHPC and the DFG through grant no INST 40/467-1 FUGG are gratefully acknowledged.

References

1. Datta, S. *Quantum Transport: Atom to Transistor*; Cambridge Univ. Press: Cambridge, 2005.
2. Cuevas, J. C.; Scheer, E. *Molecular Electronics: An Introduction to Theory and Experiment*, 2nd ed.; World Scientific, 2017; World Scientific Series in Nanoscience and Nanotechnology: Vol. 15.
3. Bâldea, I., Ed. *Molecular Electronics: An Experimental and Theoretical Approach*; Pan Stanford, 2015.
4. Fazzi, D.; Vozzi, C. In *Carbon Nanomaterials Sourcebook: Nanofibers, Nanoporous Structures, and Nanocomposites*; Sattler, K. D., Ed.; CRC Press, Boca Raton, FL, USA, 2016; Vol. 2; Chapter 2. Linear Carbon Chains, pp 27–47.

5. Goulay, F.; Trevitt, A. J.; Meloni, G.; Selby, T. M.; Osborn, D. L.; Taatjes, C. A.; Vereecken, L.; Leone, S. R. Cyclic Versus Linear Isomers Produced by Reaction of the Methylidyne Radical (CH) with Small Unsaturated Hydrocarbons. *J. Am. Chem. Soc.* **2009**, *131*, 993–1005, PMID: 19123915.
6. Smith, A. M.; Stecher, T. P. Carbon Monoxide in the Interstellar Spectrum of Zeta Ophiuchi. *Astrophys. J. Lett.* **1971**, *164*, L43.
7. Snyder, L. E.; Buhl, D. Observations of Radio Emission from Interstellar Hydrogen Cyanide. *Astrophys. J. Lett.* **1971**, *163*, L47.
8. Turner, B. E. Detection of Interstellar Cyanoacetylene. *Astrophys. J. Lett.* **1971**, *163*, L35.
9. Avery, L. W.; Broten, N. W.; MacLeod, J. M.; Oka, T.; Kroto, H. W. Detection of the Heavy Interstellar Molecule Cyanodiacetylene. *Astrophys. J. Lett.* **1976**, *205*, L173–L175.
10. Souza, S. P.; Lutz, B. L. Detection of C₂ in the Interstellar Spectrum of Cygnus OB2 Number 12/VI Cygni Number 12/. *Astrophys. J. Lett.* **1977**, *216*, L49–L51.
11. Kroto, H. W.; Kirby, C.; Walton, D. R. M.; Avery, L. W.; Broten, N. W.; MacLeod, J. M.; Oka, T. The Detection of Cyanoheptatriyne, H(C≡C)₃CN, in Heile’s Cloud 2. *Astrophys. J. Lett.* **1978**, *219*, L133–L137.
12. Broten, N. W.; Oka, T.; Avery, L. W.; MacLeod, J. M.; Kroto, H. W. The Detection of HC₉N in Interstellar Space. *Astrophys. J. Lett.* **1978**, *223*, L105–L107.
13. Matthews, H. E.; Irvine, W. M.; Friberg, P.; Brown, R. D.; Godfrey, P. D. A New Interstellar Molecule: Triearbon Monoxide. *Nature* **1984**, *310*, 125–126.
14. Hinkle, K. W.; Keady, J. J.; Bernath, P. F. Detection of C₃ in the Circumstellar Shell of IRC+10216. *Science* **1988**, *241*, 1319–1322.

15. Bernath, P. F.; Hinkle, K. H.; Keady, J. J. Detection of C5 in the Circumstellar Shell of IRC+10216. *Science* **1989**, *244*, 562–564.
16. Ohishi, M.; Suzuki, H.; Ishikawa, S.-I.; Yamada, C.; Kanamori, H.; Irvine, W. M.; Brown, R. D.; Godfrey, P. D.; Kaifu, N. Detection of a New Carbon-Chain Molecule, CCO. *Astrophys. J. Lett.* **1991**, *380*, L39–L42.
17. Guélin, M.; Cernicharo, J. Astronomical Detection of the HCCN Radical - Toward a New Family of Carbon-Chain Molecules? *Astron. Astrophys.* **1991**, *244*, L21–L24.
18. Bell, M. B.; Feldman, P. A.; Travers, M. J.; McCarthy, M. C.; Gottlieb, C. A.; Thaddeus, P. Detection of HC₁₁N in the Cold Dust Cloud TMC-1. *Astrophys. J. Lett.* **1997**, *483*, L61, See also ref. 74.
19. Cernicharo, J.; Goicoechea, J. R.; Caux, E. Far-Infrared Detection of C₃ in Sagittarius B2 and IRC +10216. *Astrophys. J. Lett.* **2000**, *534*, L199.
20. Cernicharo, J.; Guélin, M.; Pardo, J. R. Detection of the Linear Radical HC₄N in IRC +10216. *Astrophys. J. Lett.* **2004**, *615*, L145.
21. Graupner, K.; Field, T. A.; Saunders, G. C. Experimental Evidence for Radiative Attachment in Astrochemistry from Electron Attachment to NCCCCN. *Astrophys. J. Lett.* **2008**, *685*, L95.
22. Etim, E. E.; Gorai, P.; Das, A.; Chakrabarti, S. K.; Arunan, E. Systematic Theoretical Study on the Interstellar Carbon Chain Molecules. *Astrophys. J.* **2016**, *832*, 144.
23. Ref. 24 contains an explicit (and incorrect) assertion on the type of ground state (namely, singlet, *cf.* Table 1 of ref. 24). Ref. 22, a work done by the same group, does not explicitly stated what is the spin multiplicity of the state of the molecules considered but tacitly admitted singlet ground states of all cases where our results indicate triplet ground states. For more details the reader is referred to the SI.

24. Etim, E. E.; Arunan, E. Accurate Rotational Constants for Linear Interstellar Carbon Chains: Achieving Experimental Accuracy. *Astrophys. Space Sci.* **2016**, *362*, 4.
25. Fan, Q.; Pfeiffer, G. V. Theoretical Study of Linear C_n ($n=6-10$) and HC_nH ($n=2-10$) Molecules. *Chem. Phys. Lett.* **1989**, *162*, 472 – 478.
26. Wu, Z.; Xu, S.; Lu, H.; Khamoshi, A.; Liu, G.-B.; Han, T.; Wu, Y.; Lin, J.; Long, G.; He, Y.; Cai, Y.; Yao, Y.; Zhang, F.; Wang, N. Even-Odd Layer-Dependent Magnetotransport of High-Mobility Q-Valley Electrons in Transition Metal Disulfides. *Nat. Commun.* **2016**, *7*, 12955.
27. Tao, F.; Bernasek, S. L. Understanding Odd-Even Effects in Organic Self-Assembled Monolayers. *Chem. Rev.* **2007**, *107*, 1408–1453, PMID: 17439290.
28. Bâldea, I.; Köppel, H.; Cederbaum, L. S. Structural and Magnetic Transitions in Ensembles of Mesoscopic Peierls Rings in a Magnetic Flux. *Phys. Rev. B* **1999**, *60*, 6646–6654.
29. Bâldea, I.; Köppel, H.; Cederbaum, L. S. Quantum Phonon Fluctuations in Mesoscopic Dimerized Systems. *J. Phys. Soc. Jpn.* **1999**, *68*, 1954–1962.
30. Bâldea, I.; Köppel, H.; Cederbaum, L. S. Collective Quantum Tunneling of Strongly Correlated Electrons in Commensurate Mesoscopic Rings. *Eur. Phys. J. B* **2001**, *20*, 289–299.
31. Bâldea, I.; Cederbaum, L. S. Orbital Picture of Ionization and Its Breakdown in Nanoarrays of Quantum Dots. *Phys. Rev. Lett.* **2002**, *89*, 133003, selected for Virtual Journal of Nanoscale Science & Technology, **6** (12) (14 Sept, 2002).
32. Hückel, E. Quantentheoretische Beiträge zum Benzolproblem. *Z. Phys.* **1931**, *70*, 204–286.
33. Hückel, E. Quantentheoretische Beiträge zum Benzolproblem. *Z. Phys.* **1931**, *72*, 310–337.

34. Hückel, E. Quantentheoretische Beiträge zum Problem der aromatischen und ungesättigten Verbindungen. III. *Z. Phys.* **1932**, *76*, 628–648.
35. London, F. Théorie Quantique des Courants Interatomiques dans les Combinaisons Aromatiques. *J. Phys. Radium* **1937**, *8*, 397–409.
36. Frisch, M. J.; Trucks, G. W.; Schlegel, H. B.; Scuseria, G. E.; Robb, M. A.; Cheeseman, J. R.; Scalmani, G.; Barone, V.; Petersson, G. A.; Nakatsuji, H.; Li, X.; Caricato, M.; Marenich, A. V.; Bloino, J.; Janesko, B. G.; Gomperts, R.; Mennucci, B.; Hratchian, H. P.; Ortiz, J. V.; Izmaylov, A. F. *et al.* Gaussian, Inc., Wallingford CT, Gaussian 16, Revision B.01. 2016; www.gaussian.com.
37. bwHPC, bwHPC program supported by the State of Baden-Württemberg and the German Research Foundation (DFG) through grant no INST 40/467-1 FUGG. 2013; <https://www.bwhpc.de/bwhpc-c5.html>.
38. Bartlett, R. J.; Purvis, G. D. Many-Body Perturbation Theory, Coupled-Pair Many-Electron Theory, and the Importance of Quadruple Excitations for the Correlation Problem. *Int. J. Quantum Chem.* **1978**, *14*, 561–581.
39. Ochterski, J. W. Thermochemistry in Gaussian. 2000; <https://gaussian.com/wp-content/uploads/dl/thermo.pdf>, Pittsburg, PA: Gaussian Inc., url: <http://gaussian.com/wp-content/uploads/dl/thermo.pdf>.
40. Doney, K. D.; Zhao, D.; Stanton, J. F.; Linnartz, H. Theoretical Investigation of the Infrared Spectrum of Small Polyynes. *Phys. Chem. Chem. Phys.* **2018**, *20*, 5501–5508.
41. Abe, M. Diradicals. *Chem. Rev.* **2013**, *113*, 7011–7088, PMID: 23883325.
42. Cernicharo, J.; Heras, A. M.; Tielens, A. G. G. M.; Pardo, J. R.; Herpin, F.; Guélin, M.; Waters, L. B. F. M. Infrared Space Observatory’s Discovery of C₄H₂, C₆H₂, and Benzene in CRL 618. *Astrophys. J. Lett.* **2001**, *546*, L123–L126.

43. Sommerfeld, T.; Knecht, S. Electronic Interaction Between Valence and Dipole-Bound States of the Cyanoacetylene Anion. *Eur. Phys. J. D* **2005**, *35*, 207–216.
44. Graupner, K.; Merrigan, T. L.; Field, T. A.; Youngs, T. G. A.; Marr, P. C. Dissociative electron attachment to HCCCN. *New J. Phys.* **2006**, *8*, 117.
45. Bâldea, I. Long Carbon-Based Chains of Interstellar Medium Can Have a Triplet Ground State. Why Is This Important for Astrochemistry? *ACS Earth Space Chem.* **2019**, *3*, 863–872.
46. Bâldea, I. Alternation of Singlet and Triplet States in Carbon-Based Chain Molecules and Its Astrochemical Implications: Results of an Extensive Theoretical Study. *Adv. Theor. Simul.* **2019**, *2*, 1900084.
47. Cernicharo, J.; Guélin, M.; Hein, H.; Kahane, C. Sulfur in IRC + 10216. *Astron. Astrophys.* **1987**, *181*, L9–L12.
48. Agúndez, M.; Cernicharo, J.; Guélin, M. New Molecules in IRC +10216: Confirmation of C₅S and Tentative Identification of MgCCH, NCCP, and SiH₃CN. *Astron. Astrophys.* **2014**, *570*, A45.
49. Pople, J. A.; Untch, K. G. Induced Paramagnetic Ring Currents. *J. Am. Chem. Soc.* **1966**, *88*, 4811–4815.
50. Jones, R. O.; Gunnarsson, O. The Density Functional Formalism, Its Applications and Prospects. *Rev. Mod. Phys.* **1989**, *61*, 689–746.
51. Bâldea, I. Extending the Newns-Anderson Model to Allow Nanotransport Studies Through Molecules with Floppy Degrees of Freedom. *Europhys. Lett.* **2012**, *99*, 47002.
52. Bâldea, I. Transition Voltage Spectroscopy Reveals Significant Solvent Effects on Molecular Transport and Settles an Important Issue in Bipyridine-Based Junctions. *Nanoscale* **2013**, *5*, 9222–9230.

53. Bâldea, I. A Quantum Chemical Study from a Molecular Transport Perspective: Ionization and Electron Attachment Energies for Species Often Used to Fabricate Single-Molecule Junctions. *Faraday Discuss.* **2014**, *174*, 37–56.
54. Bâldea, I. Quantifying the Relative Molecular Orbital Alignment for Molecular Junctions with Similar Chemical Linkage to Electrodes. *Nanotechnology* **2014**, *25*, 455202.
55. Xie, Z.; Bâldea, I.; Demissie, A. T.; Smith, C. E.; Wu, Y.; Haugstad, G.; Frisbie, C. D. Exceptionally Small Statistical Variations in the Transport Properties of Metal-Molecule-Metal Junctions Composed of 80 Oligophenylene Dithiol Molecules. *J. Am. Chem. Soc.* **2017**, *139*, 5696–5699, PMID: 28394596.
56. Hansen, N.; Klippenstein, S. J.; Westmoreland, P. R.; Kasper, T.; Kohse-Höinghaus, K.; Wang, J.; Cool, T. A. A Combined Ab Initio and Photoionization Mass Spectrometric Study of Polyynes in Fuel-Rich Flames. *Phys. Chem. Chem. Phys.* **2008**, *10*, 366–374.
57. Li, Y.; Zhang, L.; Tian, Z.; Yuan, T.; Zhang, K.; Yang, B.; Qi, F. Investigation of the Rich Premixed Laminar Acetylene/Oxygen/Argon Flame: Comprehensive Flame Structure and Special Concerns of Polyynes. *Proc. Combust. Inst.* **2009**, *32*, 1293 – 1300.
58. Ehara, M.; Hasegawa, J.; Nakatsuji, H. In *Theory and Applications of Computational Chemistry*; Dykstra, C. E., Frenking, G., Kim, K. S., Scuseria, G. E., Eds.; Elsevier: Amsterdam, 2005; pp 1099 – 1141.
59. Christiansen, O. Coupled Cluster Theory with Emphasis on Selected New Developments. *Theor. Chem. Acc.* **2006**, *116*, 106–123.
60. White, S. R.; Martin, R. L. Ab Initio Quantum Chemistry Using the Density Matrix Renormalization Group. *J. Chem. Phys.* **1999**, *110*, 4127–4130.

61. Chan, G. K.-L.; Head-Gordon, M. Highly Correlated Calculations with a Polynomial Cost Algorithm: A Study of the Density Matrix Renormalization Group. *J. Chem. Phys.* **2002**, *116*, 4462–4476.
62. Chan, G. K.-L.; Zgid, D. In *Annu. Rep. Comput. Chem.*; Wheeler, R. A., Ed.; Elsevier, 2009; Vol. 5; pp 149 – 162.
63. The linear HC₁₀N molecule is of interest on its own that needs a separate discussion⁴⁵.
64. Ball, C. D.; McCarthy, M. C.; Thaddeus, P. Cavity Ringdown Spectroscopy of the Linear Carbon Chains HC₇H, HC₉H, HC₁₁H, and HC₁₃H. *J. Chem. Phys.* **2000**, *112*, 10149–10155.
65. Chen, X.; Steglich, M.; Gupta, V.; Rice, C. A.; Maier, J. P. Gas Phase Electronic Spectra of Carbon Chains C_n (n = 6–9). *Phys. Chem. Chem. Phys.* **2014**, *16*, 1161–1165.
66. Aoki, K.; Ikuta, S. Is a Triplet HC₄N Molecule Linear? *J. Chem. Phys.* **1993**, *98*, 7661–7662.
67. Aoki, K.; Ikuta, S.; Murakami, A. Most Stable Isomer and Singlet-Triplet Energy Separation in the HC₄N molecule. *Chem. Phys. Lett.* **1993**, *209*, 211 – 215.
68. Gutowski, M.; Skurski, P.; Boldyrev, A. I.; Simons, J.; Jordan, K. D. Contribution of Electron Correlation to the Stability of Dipole-Bound Anionic States. *Phys. Rev. A* **1996**, *54*, 1906–1909.
69. Kim, S. G.; Lee, Y. H.; Nordlander, P.; Tománek, D. Disintegration of Finite Carbon Chains in Electric Fields. *Chem. Phys. Lett.* **1997**, *264*, 345 – 350.
70. Smith, A. M.; Engel, C.; Thoma, A.; Schallmoser, G.; Wurfel, B. E.; Bondybey, V. E. Tentative Identification of C₅N₂ in Rare Gas Matrices. *Chem. Phys.* **1994**, *184*, 233 – 245.

- 71. Ohshima, Y.; Endo, Y.; Ogata, T. Fourier-Transform Microwave Spectroscopy of Triplet Carbon Monoxides, C₂O, C₄O, C₆O, and C₈O. *J. Chem. Phys.* **1995**, *102*, 1493–1500.
- 72. McGuire, B. A.; Martin-Drumel, M.-A.; Lee, K. L. K.; Stanton, J. F.; Gottlieb, C. A.; McCarthy, M. C. Vibrational satellites of C₂S, C₃S, and C₄S: Microwave Spectral Taxonomy as a Stepping Stone to the Millimeter-Wave Band. *Phys. Chem. Chem. Phys.* **2018**, *20*, 13870–13889.
- 73. Vaizert, O.; Motylewski, T.; Wyss, M.; Riaplov, E.; Linnartz, H.; Maier, J. P. The $A^3\Sigma^- - X^3\Sigma^-$ Electronic Transition of HC₆N. *J. Chem. Phys.* **2001**, *114*, 7918–7922.
- 74. Travers, M. J.; McCarthy, M. C.; Kalmus, P.; Gottlieb, C. A.; Thaddeus, P. Laboratory Detection of the Linear Cyanopolyyne HC₁₁N. *Astrophys. J.* **1996**, *469*, L65–L68.

S1 Quantum Chemical Calculations for Triplet States: Unrestricted *versus* Restricted Open Shell Approaches

Applying the unrestricted formalism to open-shell triplet states may be problematic because of the related spin contamination. The unrestricted DFT calculations done in this study (*cf.* Section 2 in the main text) posed no special problem. In all cases, we found values $\langle \mathbf{S}^2 \rangle \approx 2.15$ before annihilation of the first spin contaminant and $\langle \mathbf{S}^2 \rangle \approx 2.01$ after annihilation. As expected in view of the insignificant departure from the exact value $\langle \mathbf{S}^2 \rangle = 2$, in spot checks, we explicitly found that differences between results obtained within unrestricted (UB3LYP) and restricted open shell (ROB3LYP) calculations are altogether negligible.

Things completely change in the case of CC-calculations. For the triplet HC₉N, unrestricted CC calculations yield values (which are typical) $\langle \mathbf{S}^2 \rangle \approx 3.63$ before annihilation of the first spin contaminant and $\langle \mathbf{S}^2 \rangle \approx 4.66$ after annihilation. In view of these unacceptable values, it is not at all surprising that properties obtained within unrestricted CC calculations are unacceptable. To illustrate, (unrestricted) UCCSD calculations yielded a dipole $D = 5.586$ debye. The value obtained from (restricted open shell) ROCCSD calculations is $D \approx 7.2$ debye; it reasonably agrees with the UB3LYP/ROB3LYP-based values of $D \approx 6.8$ debye.

S2 Remarks on Previous Work Reporting Single-Triplet Alternation

As mentioned in the main text, a singlet-triplet alternation was previously²⁵ reported to occur in linear carbon (C_n , $6 \leq n \leq 10$) and hydrogen-terminated carbon (HC_nH , $2 \leq n \leq 10$) chains. Indicating the possibility that such linear molecules can have triplet ground states is certainly a remarkable finding of ref. 25. Without any polemical intention, we have to note, however, that the results obtained there were inherently limited by the level of theory (RHF with DZ or DZP basis sets) and the computational facilities available at the time it was completed.

To illustrate the *quantitative* inaccuracies of the approach of ref. 25, let us refer to the case the $HC_{11}H$ chain. At the triplet optimum, the singlet state is predicted to lie at $-\Delta_T^{RHF/DZ} = 4.348$ eV above the triplet at the optimized geometry of the latter. According to Table 2 of the main text, with the largest Pople 6-311++g(3df, 3pd) basis sets the B3LYP, CCSD, and CCSD(T) yield $\Delta_T = -0.592; -0.783; -0.717$ eV, respectively.

Concerning the results of ref. 25, we should still note that the authors themselves were aware of the fact that their RHF-based approach may be incorrect. They even pointed out that electron correlations, which escape the RHF framework, may play an essential role to correctly describe the singlet-triplet separation.

S3 Additional Data for Enthalpies of Formation

In addition to the results presented in the main text (*cf.* Tables 1, 3, 5, 7, and 9), Tables S1, S2, S3, and S4 collect results for enthalpies of formation obtained at the B3LYP/CBSB7 level of theory, CBSB7 being a standard basis set 6-311G(2d,d,p) (5D, 7F) utilized to enforce convergence to the complete basis (CBS) limit in conjunction with the CBS-QB3 protocol as implemented in GAUSSIAN 16,³⁶ the enthalpies of formation obtained within the genuine

CBS-QB3 protocol, as well as values reported in ref. 22. *We note that due to misunderstandings related to the GAUSSIAN output files these B3LYP/CBSB7-based results for enthalpies of formation were inadequately referred to as CBS-QB3-based values for $\Delta_f H_{0,RT}^0$ in Tables S1 to S4 in ref. 46.*

To demonstrate that ref. 22 implicitly (and incorrectly) took for granted that all HC_nH , HC_nN , C_nO , and C_nS possess singlet ground states, in Tables S1, S2, S3, and S4 we have also included values of those authors. The small differences between their results and our results for singlet states are due to the different methods employed to compute the enthalpies of formation. These differences are comparable to the differences from the values deduced obtained within the CBS-Q3B protocol,³⁶ as visible in the same Tables S1, S2, S3, and S4.

S4 HOMO Spatial Distributions and Cartesian Coordinates of Representative Carbon-Based Chains

Figures S1, S2, S3, S4, S5, S6, S7, S8, S9, and S10 depict HOMO spatial distributions of singlet and triplet isomers of representative carbon chains analyzed in the main text.

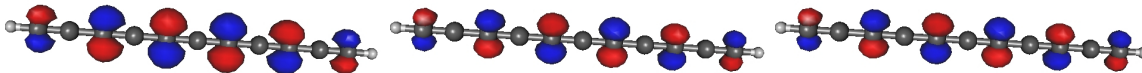


Figure S1: HOMO distributions of HC_{11}H chains. Left to right: singlet; triplet alpha; triplet beta.

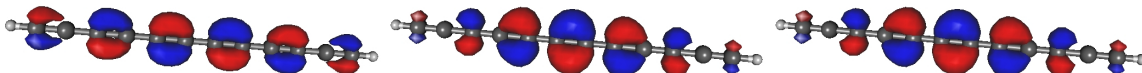


Figure S2: HOMO distributions of HC_{12}H chains. Left to right: singlet; triplet alpha; triplet beta.

The corresponding Cartesian coordinates are presented in Tables S5, S6, S7, S8, S9, S10, S11, S12, S13, S14, S15, S16, S17, S18, S19, S20, S21, S22, S23, and S24, respectively.

Table S1: Enthalpies of formation of HC_nH chains. Notice that the values of ref. 22 correspond to singlet states. (The small differences between the values obtained singlet states within the DFT/B3LYP/6-311++g(3df, 3pd) approach and those of ref. 22 are due to the different method utilized there; they are comparable to the differences from the values obtained by means of the CBS-QB3 protocol.³⁶)

Molec.	$\Delta_f H_0^0$	$\Delta_f H_{RT}^0 _S$	$\Delta_f H_0^0$	$\Delta_f H_{RT}^0 _T$
$\text{HC}_5\text{H}^\dagger$	183.280	184.472	166.461	167.299
HC_5H^*	189.935	191.144	172.182	173.169
$\text{HC}_5\text{H}^\text{N}$	193.822	198.320	175.078	179.358
$\text{HC}_5\text{H}^\ddagger$	185.283	—	—	—
$\text{HC}_6\text{H}^\dagger$	163.773	164.660	227.837	229.260
HC_6H^*	170.909	171.863	235.42	236.907
$\text{HC}_6\text{H}^\text{N}$	166.273	170.773	242.988	248.019
$\text{HC}_6\text{H}^\ddagger$	161.678	—	—	—
$\text{HC}_7\text{H}^\dagger$	229.287	231.208	212.236	213.732
HC_7H^*	237.178	239.330	220.553	222.089
$\text{HC}_7\text{H}^\text{N}$	243.944	249.893	224.401	229.74
$\text{HC}_7\text{H}^\ddagger$	226.691	—	—	—
$\text{HC}_8\text{H}^\dagger$	215.390	216.935	270.313	272.668
HC_8H^*	224.660	226.344	280.042	282.585
$\text{HC}_8\text{H}^\text{N}$	220.208	225.947	290.236	296.832
$\text{HC}_8\text{H}^\ddagger$	212.684	—	—	—
$\text{HC}_9\text{H}^\dagger$	275.106	277.356	259.606	261.482
HC_9H^*	285.570	288.076	269.797	271.871
$\text{HC}_9\text{H}^\text{N}$	293.872	300.685	273.161	279.545
$\text{HC}_{10}\text{H}^\dagger$	266.706	268.921	314.956	317.451
HC_{10}H^*	278.310	280.664	326.43	329.279
$\text{HC}_{10}\text{H}^\text{N}$	274.294	281.211	334.920	342.332
$\text{HC}_{11}\text{H}^\dagger$	322.336	325.149	307.943	310.455
HC_{11}H^*	334.832	338.981	320.16	322.979
$\text{HC}_{11}\text{H}^\text{N}$	344.598	352.556	324.389	332.026

[†] Based on the DFT/B3LYP/6-311++(3df, 3pd) approach, same as in the main text

^{*} Based on the DFT/B3LYP/CBSB7

^N CBS-QB3 protocol

[‡] From ref. 22

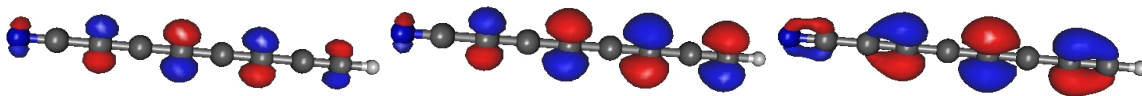


Figure S3: HOMO distributions of HC_8N chains. Left to right: singlet; triplet alpha; triplet beta.

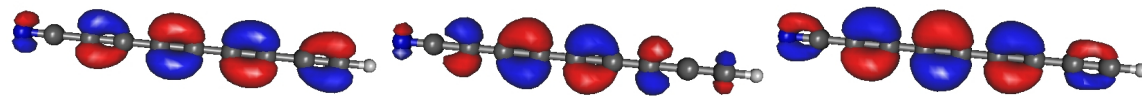


Figure S4: HOMO distributions of HC_9N chains. Left to right: singlet; triplet alpha; triplet beta.

Table S2: Enthalpies of formation of HC_nN chains. Notice that the values of ref. 22 correspond to singlet states. (The small differences between the values obtained singlet states within the DFT/B3LYP/6-311++g(3df, 3pd) approach and those of ref. 22 are due to the different method utilized there; they are comparable to the differences from the values obtained by means of the CBS-QB3 protocol.³⁶)

Molec.	$\Delta_f H_0^0$	$\Delta_f H_{RT}^0 _S$	$\Delta_f H_0^0$	$\Delta_f H_{RT}^0 _T$
$\text{HC}_4\text{N}^\dagger$	164.202	165.109	146.902	147.703
$\text{HC}_4\text{N}^\ddagger$	161.602	—	—	—
$\text{HC}_5\text{N}^\dagger$	141.802	142.735	205.424	206.859
HC_5N^*	149.434	150.348	failed to	converge
$\text{HC}_5\text{N}^\aleph$	145.889	150.124	failed to	converge
$\text{HC}_5\text{N}^\ddagger$	140.566	—	—	—
$\text{HC}_6\text{N}^\dagger$	209.099	210.827	191.840	193.150
$\text{HC}_6\text{N}^\ddagger$	211.115	—	—	—
$\text{HC}_7\text{N}^\dagger$	193.670	195.288	246.645	248.688
HC_7N^*	203.421	205.106	262.585	264.528
$\text{HC}_7\text{N}^\aleph$	200.090	205.605	272.288	278.058
$\text{HC}_7\text{N}^\ddagger$	191.824	—	—	—
$\text{HC}_8\text{N}^\dagger$	254.993	257.248	238.960	241.102
HC_8N^*	265.992	268.358	249.702	251.938
$\text{HC}_8\text{N}^\aleph$	274.618	280.994	272.288	278.058
$\text{HC}_8\text{N}^\ddagger$	263.903	—	—	—
$\text{HC}_9\text{N}^\dagger$	245.201	247.476	290.266	292.834
HC_9N^*	257.342	259.680	302.446	305.095
$\text{HC}_9\text{N}^\aleph$	254.474	261.151	309.626	316.615
$\text{HC}_9\text{N}^\ddagger$	242.928	—	—	—
$\text{HC}_{10}\text{N}^\dagger$	301.872	304.711	287.203	289.986
HC_{10}N^*	315.453	318.318	300.514	303.336
$\text{HC}_{10}\text{N}^\aleph$	326.120	333.577	305.986	313.402
$\text{HC}_{10}\text{N}^\ddagger$	317.217	—	—	—
$\text{HC}_{11}\text{N}^\dagger$	296.620	299.539	336.070	339.228
HC_{11}N^*	310.585	313.719	350.093	353.494
$\text{HC}_{11}\text{N}^\aleph$	308.204	316.186	366.987	375.329
$\text{HC}_{11}\text{N}^\ddagger$	292.191	—	—	—
$\text{HC}_{12}\text{N}^\dagger$	349.939	353.385	336.219	339.636
$\text{HC}_{12}\text{N}^\ddagger$	372.551	—	—	—

\dagger Based on the DFT/B3LYP/6-311++(3df, 3pd) approach, same as in the main text

* CBS-QB3 protocol

\ddagger From ref. 22

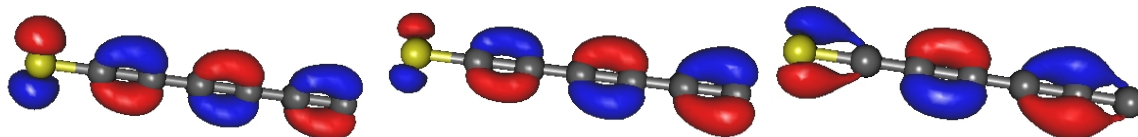


Figure S5: HOMO distributions of C_6S chains. Left to right: singlet; triplet alpha; triplet beta.

Table S3: Enthalpies of formation of C_nS chains. Notice that the values of ref. 22 correspond to singlet states. (The small differences between the values obtained singlet states within the DFT/B3LYP/6-311++g(3df, 3pd) approach and those of ref. 22 are due to the different method utilized there; they are comparable to the differences from the values obtained by means of the CBS-QB3 protocol.³⁶)

Molec.	$\Delta_f H_0^0$	$\Delta_f H_{RT S}^0$	$\Delta_f H_0^0$	$\Delta_f H_{RT T}^0$
CS [†]	70.934	69.634	146.830	147.617
CS [*]	73.630	74.411	149.652	150.440
CS ^ℵ	65.464	67.546	144.920	147.008
CS [‡]	72.404	—	—	—
C ₂ S [†]	162.418	163.565	145.630	146.834
C ₂ S [*]	167.080	168.219	150.033	151.226
C ₂ S ^ℵ	159.061	161.754	149.895	152.641
C ₂ S [‡]	141.307	—	—	—
C ₃ S [†]	135.505	136.805	190.378	191.944
C ₃ S [*]	141.215	142.514	195.902	197.456
C ₃ S ^ℵ	137.088	140.194	197.569	200.931
C ₃ S [‡]	136.292	—	—	—
C ₄ S [†]	196.846	198.489	182.693	184.308
C ₄ S [*]	203.886	205.563	189.699	191.346
C ₄ S ^ℵ	199.634	203.374	192.348	196.058
C ₄ S [‡]	196.958	—	—	—
C ₅ S [†]	191.231	193.097	232.108	234.229
C ₅ S [*]	199.412	201.276	240.452	242.625
C ₅ S ^ℵ	199.486	203.668	246.506	250.997
C ₅ S [‡]	190.684	—	—	—
C ₆ S [†]	243.319	245.553	232.214	234.417
C ₆ S [‡]	253.179	255.336	241.955	244.109
C ₆ S [‡]	254.207	—	—	—
C ₇ S [†]	245.291	247.800	276.777	279.455
C ₇ S [*]	255.720	258.298	290.27	293.178
C ₇ S ^ℵ	259.573	264.977	291.448	297.183
C ₇ S [‡]	243.788	—	—	—

[†] Based on the DFT/B3LYP/6-311++(3df, 3pd) approach, same as in the main text

^{*} B3LYP/CBSB7

^ℵ CBS-QB3 protocol

[‡] From ref. 22

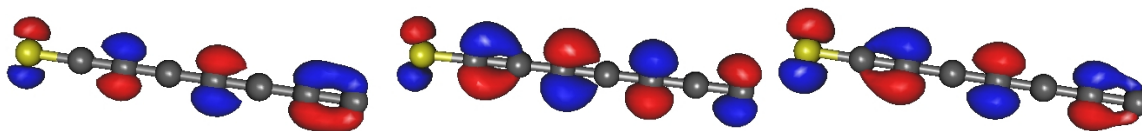


Figure S6: HOMO distributions of C_7S chains. Left to right: singlet; triplet alpha; triplet beta.

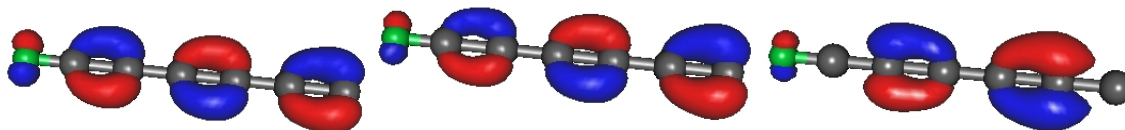


Figure S7: HOMO distributions of C_6O chains. Left to right: singlet; triplet alpha; triplet beta.

Table S4: Enthalpies of formation of C_nO chains. Notice that the values of ref. 22 correspond to singlet states. (The small differences between the values obtained singlet states within the DFT/B3LYP/6-311++g(3df, 3pd) approach and those of ref. 22 are due to the different method utilized there; they are comparable to the differences from the values obtained by means of the CBS-QB3 protocol.³⁶)

Molec.	$\Delta_f H_0^0$	$\Delta_f H_{RT}^0 _S$	$\Delta_f H_0^0$	$\Delta_f H_{RT}^0 _T$
CO [†]	-24.140	-23.356	110.602	111.387
CO [‡]	-23.127	—	—	—
C ₂ O [†]	110.227	111.332	85.497	86.550
C ₂ O [‡]	91.369	—	—	—
C ₃ O [†]	76.170	77.389	143.236	144.734
C ₃ O [‡]	75.328	—	—	—
C ₄ O [†]	149.118	150.669	133.039	134.532
C ₄ O [*]	154.374	149.427	138.648	140.212
C ₄ O ^ℵ	153.646	157.480	145.245	148.862
C ₄ O [‡]	148.640	—	—	—
C ₅ O [†]	135.765	137.516	186.814	188.994
C ₅ O [*]	142.551	144.386	193.213	196.975
C ₅ O ^ℵ	145.935	150.076	202.711	207.499
C ₅ O [‡]	133.782	—	—	—
C ₆ O [†]	193.343	195.458	181.261	183.327
C ₆ O [*]	201.115	203.454	189.021	191.305
C ₆ O ^ℵ	203.944	208.844	198.524	203.370
C ₆ O [‡]	204.526	—	—	—

[†] Based on the DFT/B3LYP/6-311++(3df, 3pd) approach, same as in the main text

^{*} B3LYP/CBSB7

^ℵ CBS-QB3 protocol

[‡] From ref. 22

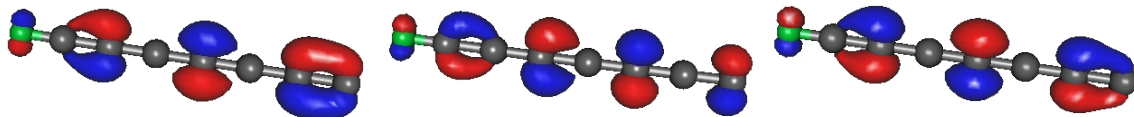


Figure S8: HOMO distributions of C_7O chains. Left to right: singlet; triplet alpha; triplet beta.

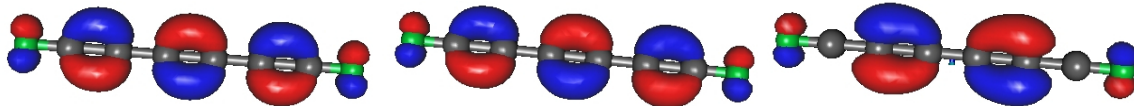


Figure S9: HOMO distributions of OC_6O chains. Left to right: singlet; triplet alpha; triplet beta.

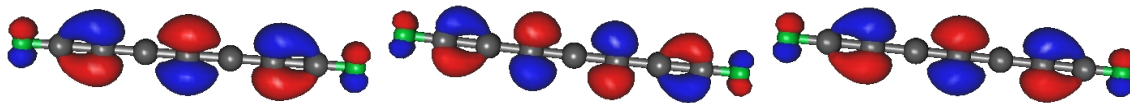


Figure S10: HOMO distributions of OC_7O chains. Left to right: singlet; triplet alpha; triplet beta.

Table S5: Geometry of a singlet HC₁₁H chain optimized at DFT/B3LYP/6-311++g(3df, 3pd) level. All coordinates in angstrom.

Atom	X	Y	Z
H	0.00000000	0.00000000	7.42219600
C	0.00000000	0.00000000	6.36073600
C	0.00000000	0.00000000	5.14476600
C	0.00000000	0.00000000	3.81191600
C	0.00000000	0.00000000	2.56889600
C	0.00000000	0.00000000	1.26974600
C	0.00000000	0.00000000	0.00001600
C	0.00000000	0.00000000	-1.26971400
C	0.00000000	0.00000000	-2.56886400
C	0.00000000	0.00000000	-3.81187400
C	0.00000000	0.00000000	-5.14473400
C	0.00000000	0.00000000	-6.36085400
H	0.00000000	0.00000000	-7.42243400

Table S6: Geometry of a triplet HC₁₁H chain optimized at DFT/B3LYP/6-311++g(3df, 3pd) level. All coordinates in angstrom.

Atom	X	Y	Z
H	7.42392900	0.21171400	0.06333600
C	6.36288700	0.18177100	0.05413900
C	5.14726900	0.14738000	0.04354300
C	3.81387300	0.10951800	0.03186600
C	2.57049600	0.07395900	0.02112100
C	1.27053900	0.03655400	0.01010800
C	0.00007100	-0.00006400	-0.00053200
C	-1.27067200	-0.03670000	-0.01098800
C	-2.57038800	-0.07391900	-0.02168300
C	-3.81395000	-0.10939700	-0.03191100
C	-5.14723200	-0.14726200	-0.04290600
C	-6.36289500	-0.18177400	-0.05294200
H	-7.42391600	-0.21210500	-0.06223100

Table S7: Geometry of a singlet HC₁₂H chain optimized at DFT/B3LYP/6-311++g(3df, 3pd) level. All coordinates in angstrom.

Atom	X	Y	Z
H	0.00000000	0.00000000	-8.06870600
C	0.00000000	0.00000000	-7.00712700
C	0.00000000	0.00000000	-5.79877900
C	0.00000000	0.00000000	-4.44974900
C	0.00000000	0.00000000	-3.22901600
C	0.00000000	0.00000000	-1.89190900
C	0.00000000	0.00000000	-0.66724600
C	0.00000000	0.00000000	0.66723600
C	0.00000000	0.00000000	1.89189900
C	0.00000000	0.00000000	3.22900900
C	0.00000000	0.00000000	4.44973600
C	0.00000000	0.00000000	5.79879100
C	0.00000000	0.00000000	7.00715000
H	0.00000000	0.00000000	8.06872600

Table S8: Geometry of a triplet HC₁₂H chain optimized at DFT/B3LYP/6-311++g(3df, 3pd) level. All coordinates in angstrom.

Atom	X	Y	Z
H	0.01152900	-8.06549200	0.00000000
C	0.01077900	-7.00401500	0.00000000
C	0.00890100	-5.78238000	0.00000000
C	0.00726400	-4.45795200	0.00000000
C	0.00565600	-3.20353000	0.00000000
C	0.00394400	-1.91363900	0.00000000
C	0.00208400	-0.63883700	0.00000000
C	0.00000000	0.63882000	0.00000000
C	-0.00225500	1.91367300	0.00000000
C	-0.00483300	3.20347200	0.00000000
C	-0.00748200	4.45798000	0.00000000
C	-0.01045400	5.78235100	0.00000000
C	-0.01292200	7.00404500	0.00000000
H	-0.01562000	8.06556500	0.00000000

Table S9: Geometry of a singlet HC₈N chain optimized at DFT/B3LYP/6-311++g(3df, 3pd) level. All coordinates in angstrom.

Atom	X	Y	Z
H	0.000000	0.000000	0.000000
C	0.000000	0.000000	1.061990
C	0.000000	0.000000	2.281660
C	0.000000	0.000000	3.605300
C	0.000000	0.000000	4.860230
C	0.000000	0.000000	6.141510
C	0.000000	0.000000	7.433850
C	0.000000	0.000000	8.678190
C	0.000000	0.000000	10.017590
N	0.000000	0.000000	11.184290

Table S10: Geometry of a triplet HC₈N chain optimized at DFT/B3LYP/6-311++g(3df, 3pd) level. All coordinates in angstrom.

Atom	X	Y	Z
H	0.000000	0.000000	0.050499
C	0.000000	0.000000	1.112529
C	0.000000	0.000000	2.332695
C	0.000000	0.000000	3.657696
C	0.000000	0.000000	4.914141
C	0.000000	0.000000	6.197112
C	0.000000	0.000000	7.491184
C	0.000000	0.000000	8.736581
C	0.000000	0.000000	10.077249
N	0.000000	0.000000	11.243844

Table S11: Geometry of a singlet HC₉N chain optimized at DFT/B3LYP/6-311++g(3df, 3pd) level. All coordinates in angstrom.

Atom	X	Y	Z
H	0.000000	0.000000	0.008778
C	0.000000	1.061980	0.786078
C	0.000000	2.269590	-0.127671
C	0.000000	3.618640	-0.345776
C	0.000000	4.838020	-0.158290
C	0.000000	6.176670	-0.035931
C	0.000000	7.398190	-0.589738
C	0.000000	8.737740	-0.384900
C	0.000000	9.954280	1.087742
C	0.000000	11.310900	0.917371
N	0.000000	12.469730	-1.157929

Table S12: Geometry of a triplet HC₉N chain optimized at DFT/B3LYP/6-311++g(3df, 3pd) level. All coordinates in angstrom.

Atom	X	Y	Z
H	0.00000000	0.00000000	-6.76924400
C	0.00000000	0.00000000	-5.70728200
C	0.00000000	0.00000000	-4.48002200
C	0.00000000	0.00000000	-3.16567800
C	0.00000000	0.00000000	-1.89896700
C	0.00000000	0.00000000	-0.61966900
C	0.00000000	0.00000000	0.66054500
C	0.00000000	0.00000000	1.94595700
C	0.00000000	0.00000000	3.20223100
C	0.00000000	0.00000000	4.53430900
N	0.00000000	0.00000000	5.70581400

Table S13: Geometry of a singlet C₆S chain optimized at DFT/B3LYP/6-311++g(3df, 3pd) level. All coordinates in angstrom.

Atom	X	Y	Z
S	0.006105	0.000000	-0.019989
C	-0.017097	0.000000	1.538551
C	-0.036489	0.000000	2.812844
C	-0.056990	0.000000	4.092023
C	-0.078528	0.000000	5.361258
C	-0.101160	0.000000	6.651218
C	-0.124958	0.000000	7.937546

Table S14: Geometry of a triplet C₆S chain optimized at DFT/B3LYP/6-311++g(3df, 3pd) level. All coordinates in angstrom.

Atom	X	Y	Z
S	0.018284	0.000000	-0.218962
C	-0.015319	0.000000	1.339322
C	-0.042451	0.000000	2.612196
C	-0.064440	0.000000	3.890524
C	-0.084996	0.000000	5.159442
C	-0.102917	0.000000	6.447847
C	-0.117813	0.000000	7.736118

Table S15: Geometry of a singlet C₇S chain optimized at DFT/B3LYP/6-311++g(3df, 3pd) level. All coordinates in angstrom.

Atom	X	Y	Z
S	-0.28823100	-3.87957200	0.00000000
C	-0.18370000	-2.33341100	0.00000000
C	-0.09512400	-1.05962500	0.00000000
C	0.00000000	0.20359900	0.00000000
C	0.09921500	1.47934800	0.00000000
C	0.20525100	2.73702600	0.00000000
C	0.31500700	4.02367400	0.00000000
C	0.42796800	5.29491500	0.00000000

Table S16: Geometry of a triplet C₇S chain optimized at DFT/B3LYP/6-311++g(3df, 3pd) level. All coordinates in angstrom.

Atom	X	Y	Z
S	-0.31032700	-3.89879800	0.00000000
C	-0.19554500	-2.33684200	0.00000000
C	-0.09954800	-1.06757700	0.00000000
C	0.00000000	0.21110900	0.00000000
C	0.10794000	1.47994100	0.00000000
C	0.21939900	2.75289600	0.00000000
C	0.33716200	4.03332100	0.00000000
C	0.45812900	5.32394700	0.00000000

Table S17: Geometry of a singlet C₆O chain optimized at DFT/B3LYP/6-311++g(3df, 3pd) level. All coordinates in angstrom.

Atom	X	Y	Z
O	0.002680	0.000000	0.114732
C	-0.015651	0.000000	1.276918
C	-0.035540	0.000000	2.558251
C	-0.056544	0.000000	3.832815
C	-0.078556	0.000000	5.105768
C	-0.101140	0.000000	6.393987
C	-0.124900	0.000000	7.684016

Table S18: Geometry of a triplet C₆O chain optimized at DFT/B3LYP/6-311++g(3df, 3pd) level. All coordinates in angstrom.

Atom	X	Y	Z
O	0.002724	0.000000	0.117263
C	-0.015703	0.000000	1.278675
C	-0.035436	0.000000	2.559020
C	-0.056574	0.000000	3.832259
C	-0.078895	0.000000	5.104970
C	-0.101211	0.000000	6.390915
C	-0.124557	0.000000	7.683385

Table S19: Geometry of a singlet C₇O chain optimized at DFT/B3LYP/6-311++g(3df, 3pd) level. All coordinates in angstrom.

Atom	X	Y	Z
O	-0.001655	0.000000	0.141663
C	-0.015703	0.000000	1.298554
C	-0.031158	0.000000	2.579403
C	-0.053075	0.000000	3.842831
C	-0.077053	0.000000	5.121938
C	-0.106141	0.000000	6.383257
C	-0.137515	0.000000	7.673639
C	-0.171432	0.000000	8.948957

Table S20: Geometry of a triplet C₇O chain optimized at DFT/B3LYP/6-311++g(3df, 3pd) level. All coordinates in angstrom.

Atom	X	Y	Z
O	-0.000261	0.000000	0.116937
C	-0.015705	0.000000	1.282603
C	-0.032391	0.000000	2.564654
C	-0.052477	0.000000	3.841826
C	-0.077757	0.000000	5.119130
C	-0.104794	0.000000	6.397322
C	-0.137602	0.000000	7.683077
C	-0.172746	0.000000	8.984692

Table S21: Geometry of a singlet OC₆O chain optimized at DFT/B3LYP/6-311++g(3df, 3pd) level. All coordinates in angstrom.

Atom	X	Y	Z
O	0.000000	0.000000	0.001750
C	0.000000	0.000000	1.169089
C	0.000000	0.000000	2.447533
C	0.000000	0.000000	3.725728
C	0.000000	0.000000	5.000070
C	0.000000	0.000000	6.278262
C	0.000000	0.000000	7.556708
O	0.000000	0.000000	8.724060

Table S22: Geometry of a triplet OC₆O chain optimized at DFT/B3LYP/6-311++g(3df, 3pd) level. All coordinates in angstrom.

Atom	X	Y	Z
O	0.002724	0.000000	0.117263
C	-0.015703	0.000000	1.278675
C	-0.035436	0.000000	2.559020
C	-0.056574	0.000000	3.832259
C	-0.078895	0.000000	5.104970
C	-0.101211	0.000000	6.390915
C	-0.124557	0.000000	7.683385

Table S23: Geometry of a singlet OC_7O chain optimized at DFT/B3LYP/6-311++g(3df, 3pd) level. All coordinates in angstrom.

Atom	X	Y	Z
O	-0.003872	0.000000	0.028377
C	-0.015441	0.000000	1.190634
C	-0.027672	0.000000	2.466546
C	-0.050153	0.000000	3.737453
C	-0.073579	0.000000	5.009382
C	-0.107730	0.000000	6.281028
C	-0.142310	0.000000	7.551702
C	-0.187463	0.000000	8.826846
O	-0.229527	0.000000	9.988413

Table S24: Geometry of a triplet OC_7O chain optimized at DFT/B3LYP/6-311++g(3df, 3pd) level. All coordinates in angstrom.

Atom	X	Y	Z
O	-0.002686	0.000000	-0.000267
C	-0.015854	0.000000	1.170323
C	-0.029398	0.000000	2.450417
C	-0.047195	0.000000	3.730650
C	-0.074833	0.000000	5.009334
C	-0.104782	0.000000	6.287989
C	-0.144252	0.000000	7.567748
C	-0.188919	0.000000	8.847124
O	-0.229828	0.000000	10.017062

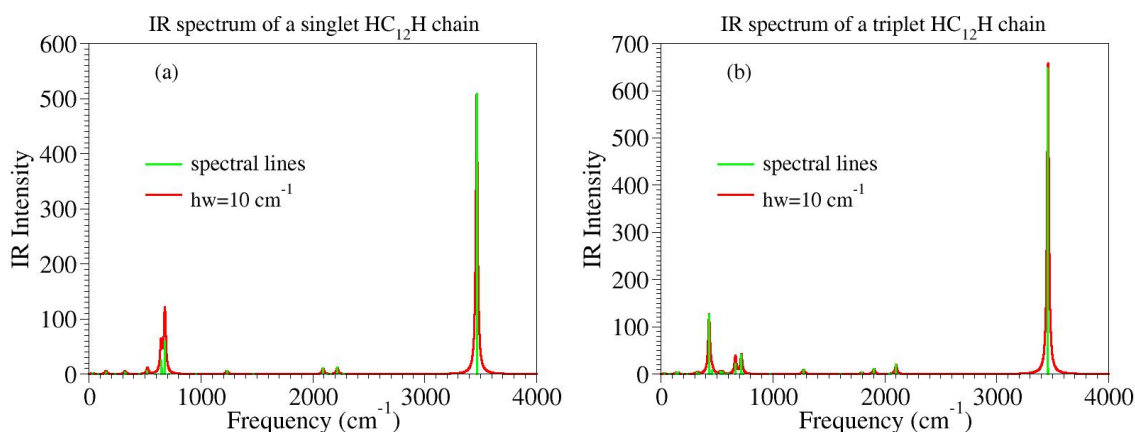


Figure S11: Infrared spectra of (a) singlet and (b) triplet HC_{12}H chains. The solid red lines were deduced by convoluting the spectral lines (depicted in green) computed within a DFT/B3LYP/6-311++g(3df, 3pd) approach by using Lorentzian distributions whose halfwidth (hw) is indicated in the legend.

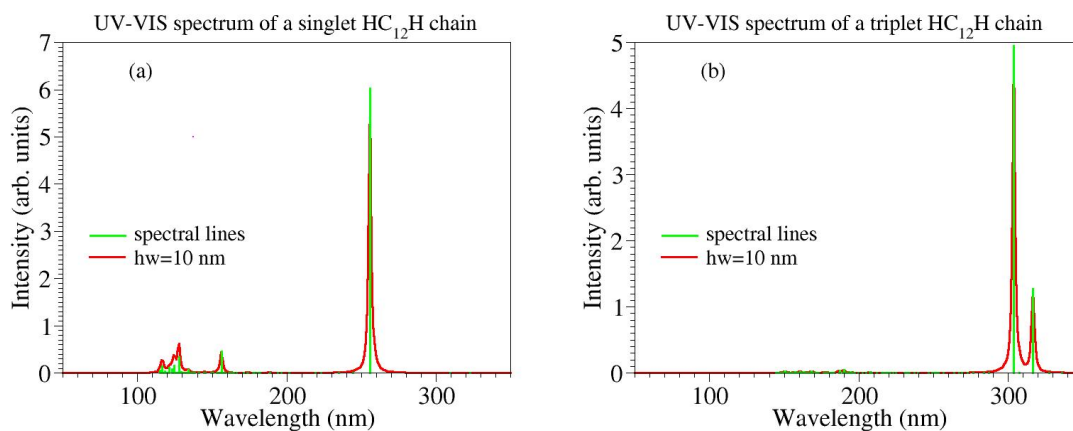


Figure S12: UV-visible absorption spectra of (a) singlet and (b) triplet HC₁₂H chains. The solid red lines were deduced by convoluting the spectral lines (depicted in green) computed within a TD-DFT/CAM-B3LYP/6-311++g(3df, 3pd) approach by using Lorentzian distributions whose halfwidth (hw) is indicated in the legend.